DETECTive: Machine Learning-driven Automatic Test Pattern Prediction for Faults in Digital Circuits

climate

MDPI

Article

Flood Damage Risk Mapping Along the River Niger: Ten Benefits of a Participated Approach

Maurizio Tiepolo [1,*], Muhammad Abraiz [2], Maurizio Bacci [3], Ousman Baoua [4], Elena Belcore [2], Giorgio Cannella [1], Edoardo Fiorillo [5], Daniele Ganora [2], Mohammed Ibrahim Housseini [6], Gaptia Lawan Katiellou [4], Marco Piras [2], Francesco Saretto [2] and Vieri Tarchiani [3]

[1] Interuniversity Department of Regional and Urban Studies and Planning, Politecnico di Torino, Viale Pier Andrea Mattioli 39, 10125 Turin, Italy; giorgio.cannella@polito.it
[2] Department of Environmental, Land and Infrastructure Engineering, Politecnico di Torino, Corso Duca degli Abruzzi 24, 10129 Turin, Italy; muhammad.abraiz@polito.it (M.A.); elena.belcore@polito.it (E.B.); daniele.ganora@polito.it (D.G.); marco.piras@polito.it (M.P.); francesco.saretto@polito.it (F.S.)
[3] Istituto per la BioEconomia, Consiglio Nazionale delle Ricerche, Via Giovanni Caproni 8, 50145 Florence, Italy; maurizio.bacci@ibe.cnr.it (M.B.); vieri.tarchiani@ibe.cnr.it (V.T.)
[4] Direction de la Météorologie Nationale du Niger, 8 Rue du Grand Hotel, Niamey BP 218, Niger; ousmanebaoua@meteo-niger.org (O.B.); katiellou.lawan@meteo-niger.org (G.L.K.)
[5] Istituto per la BioEconomia, Consiglio Nazionale delle Ricerche, Via Piero Gobetti 101, 40129 Bologna, Italy; edoardo.fiorillo@ibe.cnr.it
[6] Directorate of Water Resources, Ministry of Hydraulics, Sanitation, and Environment, Niamey BP 257, Niger; housseiniibrahimmohamed@yahoo.fr
* Correspondence: maurizio.tiepolo@polito.it

Abstract: Flood risk mapping is spreading in the Global South due to the availability of high-resolution/high-frequency satellite imagery, volunteered geographic information, and hydraulic models. However, these maps are increasingly generated without the participation of exposed communities, contrary to the Sendai Framework for Disaster Risk Reduction 2015–2030 priorities. As a result, the understanding of risk is limited. This study aims to map flood risk with citizen science complemented by hydrology, geomatics, and spatial planning. The Niger River floods of 2024–2025 on a 113 km^2 area upstream of Niamey are investigated. The novelty of the work is the integration of local and technical knowledge in the micro-mapping of risk in a large area. We consider risk the product of a hazard and damage in monetary terms. Focus groups in flooded municipalities, interviews with irrigation perimeter managers, and statistical river flow and rainfall analysis identified the hazard. The flood plain was extracted from Sentinel-2 images using MNDWI and validated with ground control points. Six classes of assets were identified by visual photo interpretation of very high-resolution satellite imagery. Damage was ascertained through interviews with a sample of farmers. The floods of 2024–2025 may occur again in the next 12–19 years. Farmers cannot crop safer sites, raising significant environmental justice issues. Damage depends on the strength of the levees, the crop, and the season. From January to February, horticulture is at a higher risk. Flooding does not bring benefits. Risk maps highlight hot spots, are validated, and can be linked to observed flood levels.

Keywords: community participation; flood damage; flood risk map; horticulture; local knowledge; MNDWI; multi-hazard; paddy fields; risk management; Sentinel-2

Academic Editor: Wen Cheng Liu

Received: 22 March 2025
Revised: 10 April 2025
Accepted: 12 April 2025
Published: 14 April 2025

Citation: Tiepolo, M.; Abraiz, M.; Bacci, M.; Baoua, O.; Belcore, E.; Cannella, G.; Fiorillo, E.; Ganora, D.; Housseini, M.I.; Katiellou, G.L.; et al. Flood Damage Risk Mapping Along the River Niger: Ten Benefits of a Participated Approach. *Climate* **2025**, *13*, 80. https://doi.org/10.3390/cli13040080

1. Introduction

Flood exposure in Sub-Saharan Africa has increased in recent years [1]. More frequent heavy rainfall on already saturated or barren soils increases runoff, feeds rivers with often

silted-up beds, and turns into floods [2–5]. Incessant demographic pressure has extended settlements and crops into flood-prone zones. According to the Sendai Framework for Disaster Risk Reduction, understanding risk is the first priority, and to achieve it locally, it is important to develop risk maps [6].

Rapid mapping is today's most widely used way to determine flood zones. It is offered on a global scale just after a disaster and without ground truth by several organizations, including UNOSAT, which has been working in support of the United Nations since 2003, Copernicus Emergency Management Service Rapid Mapping of the European Union (since 2012), and SERTIT-Service Régional de Traitement d'Image et de Télédétection of the University of Strasbourg (since 2015). Rapid mapping uses different input data and techniques [7,8]. The Modified Normalized Difference Water Index (MNDWI) extracts the flood plain from satellite images. The maps are supplemented by the road network, place names, and utilities freely provided by volunteered geographical information. Concerning flood impacts, rapid mapping extracts population density from WorldPop gridded population datasets and agriculture, vegetation, and built-up land cover from satellite images. However, the duration of the flood was not considered despite being one damage determinant. Nor was the phenological stage of crops considered. Rapid mapping is widely practiced in Asia. South of the Sahara, it is less common and favors individual watersheds or small areas [9–29].

Risk mapping was added to rapid mapping following catastrophic floods in the United States and Central Europe [30,31]. Maps determine risk as a product of hazard, exposure, and vulnerability; indicators measure each determinant, and risk is expressed according to a qualitative scale (high to low). Hazard, for example, is determined by indicators of flood triggers such as slope, flow accumulation, land cover, soil type, and precipitations. However, only 10% of the works expressed hazard as a statistical probability of occurrence [32–57]. River flow records could be used to estimate the flood frequency curve of flood peaks. However, the magnitude of recent floods has highlighted that statistics should be updated, and events once considered extraordinary are becoming much more frequent. The maps do not highlight the highest risk assets. At best, the risk level by administrative jurisdiction is extracted [44,46,48]. Risk mapping soon spread to Asia, but more rarely south of the Sahara (Table A2).

In parallel, quantitative risk assessment models were developed, such as HAZUS multi-hazards by the Federal Emergency Management Agency in the US. Models consider the hazard and potential damage expressed in monetary terms per unit area [58]. These models have had less reverberation in the Global South. The lack of input data is probably among the most important reasons. Flood depth-damage curves for specific buildings and crops in the Global South are rarely available. Land registers are missing. Detailed land-use mapping does not capture essential assets, such as horticulture, which in many rural regions is the livelihood of local communities.

Despite these limitations, quantitative risk mapping remains invaluable for estimating potential damage, damage after a disaster [59], and the cost/benefit of risk reduction [60]. Due to the context of urgency in which flood maps are produced and the large scale at which they are represented, flood rapid maps and risk mapping are top-down products. Without ground validation and the involvement of exposed communities in 75% of cases (Table A2), maps prepared so far have had an indeterminate accuracy and are of little use for local flood prevention. Consequently, genuine flood risk mapping in the South of the Sahara and, in many cases, in the Global South is lacking, especially in rural areas.

Citizen science could improve risk mapping [61]. The problem is developing participatory, damage-based, quantitative flood risk mapping. This raises a research question: How can local and technical knowledge enhance the understanding of risk provided so far

by risk mapping? Current flood risk mapping will not contribute to risk management if this question remains unanswered.

Therefore, this study aims to develop an expeditious approach to river flood risk mapping based on local knowledge supplemented by hydrological analysis, satellite-based mapping, and spatial planning within a standardized risk management process [62,63]. We hypothesize that early participation, targeted and coordinated ground investigations, hydrological analysis, remote sensing, and planning may allow local communities to update and appropriate more accurate risk mapping.

This study is novel in integrating local and technical knowledge into flood risk micro mapping over a large area with a method that is easy to transfer to other contexts.

We will proceed with the study area's presentation and the methodology's description. The mapping results will highlight the contribution of local and technical knowledge. The discussion will answer the research question and highlight the results' implications, limitations, and recommendations. The conclusions will recall the more general significance of this work and possible developments.

2. Materials and Methods

2.1. Study Area

The study area is located along the Niger River, in its medium watershed, from its confluence with the right-bank tributary Dargol to the gates of Niamey. The Dargol and the Sirba rivers have intermittent flow on the right bank during the rainy season. On the left bank, the drainage network is characterized by small endorheic watersheds with a minimal contribution to the Niger flow (Figure 1).

The climate in the study area is determined by the West African monsoon, which has a unimodal rainy season from June to September. According to the Köppen–Geiger classification, the area is hot semi-arid (BSh). The vegetation is characterized by dry savannah and sparse bush undergoing intense deforestation [64]. Irrigated agriculture is developed in large rice-perimeters with total water control (Amenagement Hydro Agricoles or AHA, according to the French acronym), in vast horticultural sites, and in small plots cultivated with rice and vegetables. Elsewhere, rain-fed millet (*Pennisetum glaucum*) is the dominant culture, often associated with cowpea (*Vigna ungulata*) or groundnut (*Arachis hypogaea*).

Two annual floods characterize the hydrological behavior of the Niger River. The local flood occurring during the wet season between June and October is driven by the inflow of the tributaries upstream of Niamey, predominantly the Sirba River. The Guinean flood from November to February is caused by rainfall in Guinea and Mali. The area investigated belongs administratively to the municipalities of Gotheye, Karma, Kourteye, and Namaro and has 21 settlements, 1203 ha of AHA, and 1353 ha of other irrigated crops.

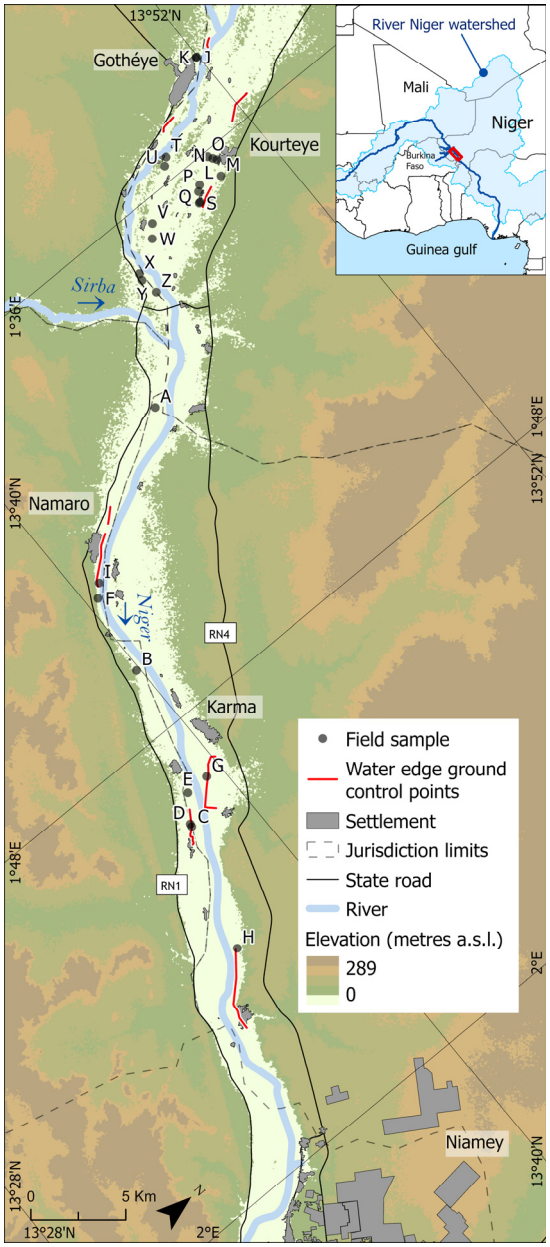

Figure 1. The study area.

2.2. Conceptual Framework

This study is contextualized against 50 rapid flood and risk mapping works developed in the Global South over the past two decades. The literature was identified through a systematic keyword search on Google Scholar (Tables A1 and A2). Flood risk (R) was considered as the product of hazard (H) and damages (D), R = H × D, according to an established conceptual framework [65–67]. We adopted a post-disaster approach and a quantitative method [68], the application of which required a combination of local and technical knowledge [69]. Local and central stakeholders participated from the very beginning of the risk mapping, helping to define the methodology, providing information, describing the dynamics, interpreting them, and validating the results obtained remotely.

2.3. Hazard

The hazard was identified through focus groups with riparian municipalities (Table A3) and interviews with the managers of AHAs (Table A4). These meetings showed that the flood was triggered by heavy rainfall and river overflow.

The fluvial flood hazard was analyzed separately for the local (or Sahelian) and Guinean floods [70]. This study considered the hydrological year that began on 1 June 2024 and was characterized by the Niger River floods that peaked on 21 August 2024 (2438 m^3/s) and 16 February 2025 (2215 m^3/s) for the local and the Guinean flood, respectively. The probability of occurrence of these floods was estimated through a statistical analysis of the maximum annual flow rates of the Niger River as observed at the Niamey station. Flow rates were calculated from water level records, referred to as "water stage" in the following figures, and the rating curves were established in 1975, 2008, and 2016 (Figure 2); rating curves were provided by the Directorate of Water Resources (Ministry of Hydraulics, Sanitation and Environment of Niger) in numerical format, while the latter is also available in analytical form [70].

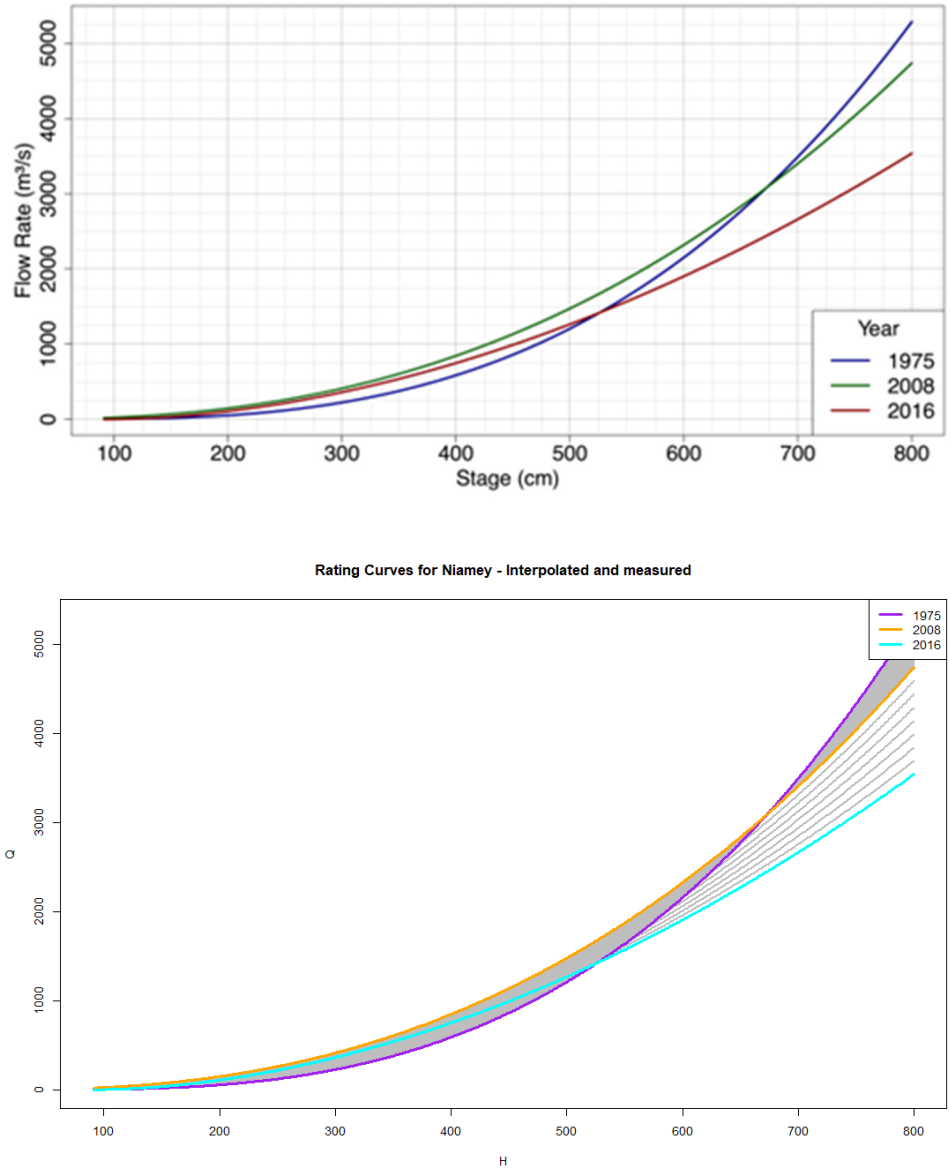

Figure 2. Graphical representation of the available rating curves (source: Directorate of Water Resources, Ministry of Hydraulics, Sanitation and Environment of Niger).

Given the absence of known rating curves for the intermediate periods, yearly rating curves were reconstructed by smoothly interpolating the available ones to transform level observations into discharge values for 1975–2015. The 2016 rating curve was considered constant for recent years, while observations before 1975 were not considered. The annual

maxima have been affected by an upward trend since the mid-1980s. Therefore, the series was treated by removing the linear trend and renormalizing it to the average of the last five years. Although more complex trends have been hypothesized to model past flood patterns [70], this work adopted simple but effective correction that allowed standard flood frequency analysis [71] under the hypothesis that recent conditions will become stable. This approach provides a robust and operational method to evaluate the flood frequency (see the function parameterization in Table A5), as well as to compute possible design values; it avoids more complex parametrization that would in-crease prediction uncertainty. Figure 3 shows the original record of local and Guinean peaks and the detrended series.

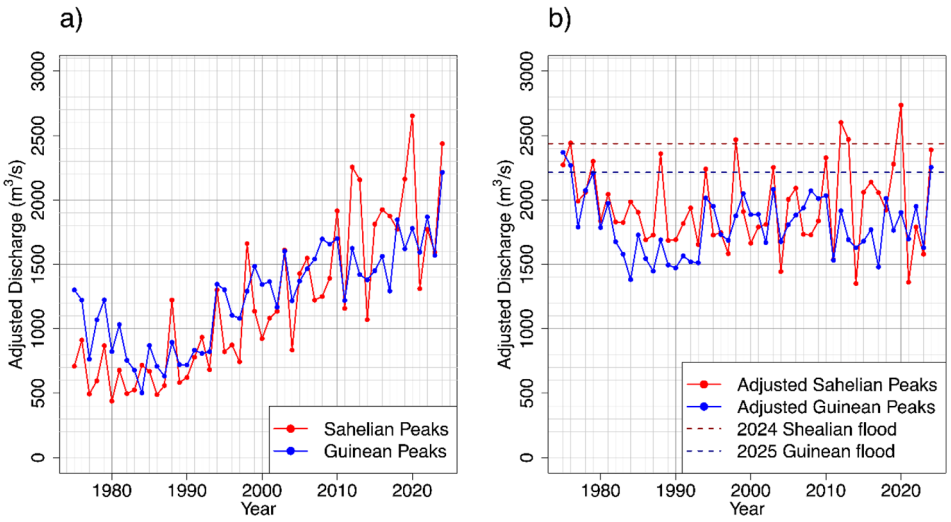

Figure 3. Historical series of annual maxima of the Niger River in Niamey (**a**) after removing the linear trend (**b**).

Based on the detrended records, the peaks' distribution was fitted with the Generalized Extreme Value distribution (GEV), commonly used in flood frequency analysis and already adopted [70], under the hypothesis that the two processes can be considered independent. The distribution parameters are estimated using the L-moment method [72,73]. The two flood frequency curves (confidence bands computed with Monte Carlo simulations), based on the approach of Laio et al. [74], allowed us to estimate the return time of the local and Guinean floods (Figure 4).

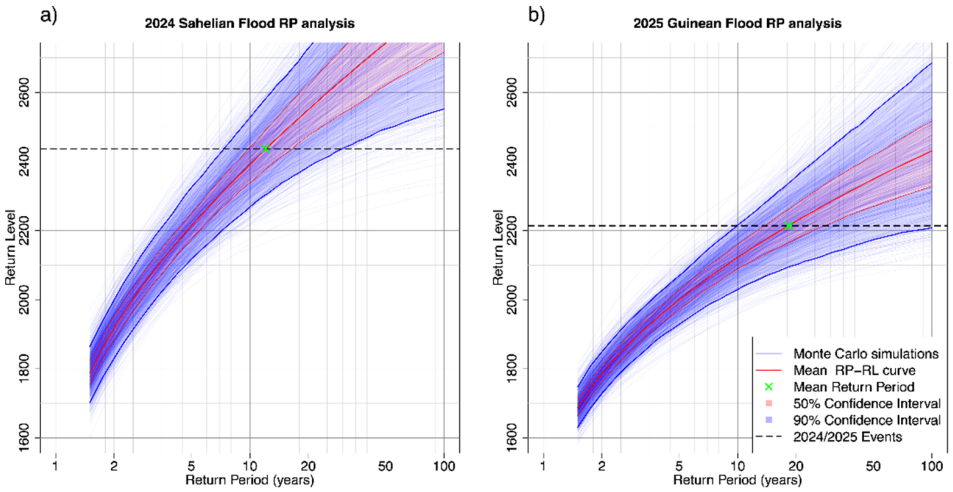

Figure 4. GEV frequency distribution with 50% and 90% confidence bands for the local flood (**a**) and Guinean (**b**). The dashed lines correspond to the recent 2024/2025 flood events.

Besides fluvial inundation, the Sahel is sensitive to pluvial extremes; recent storms (August 2024) in Namaro and Karma, with intensities of 63 mm/day and 60 mm/day, produced relevant damages. The return time of these events was evaluated based on 30 years of available daily precipitation records in Namaro. To do this, the frequency curve of extreme daily precipitation has been estimated using the Metastatistical Extreme Value distribution (MEV) [75]. This distribution considers all the daily observations above 1 mm, minimizing information exploitation and thus providing more robust results (Table A5).

2.4. Damage

Damage estimation adapts to the micro-scale of the HAZUS-MH model [58], which was designed for the meso scale. Only tangible damage that can be estimated in monetary terms is considered. Damage estimation was based on flood extent and duration related to crop phenological stage as ascertained on 24 sample fields and compared with stage-damage curves [76].

2.4.1. Flood Plain

Relating satellite imagery of the area of interest near the peak [77] to the water level and flow rate of the river in Niamey allows each image to be assigned a return time and, hence, a flood probability. The flood plain is delineated from Sentinel-2, level 2A, images taken on 16/02/2025 (H 637 cm) and 20/08/2024 (H 672 cm) accessed by Google Earth Engine (GEE) (Table 1).

Table 1. Satellite imagery.

Type	Acquisition Date	Green Band Resolution m	Infrared Band Resolution m
Sentinel 2 (2-A level)	20 August 2024	10	20
Sentinel 2 (2-A level)	16 February 2025	10	20

Green (Sentinel Band 3) and Short Wave Infrared (SWIR, Sentinel Band 11) bands were used to identify water. MNDWI calculates the normalized differences between the green and Short Wave Infrared RGB Composite (SWIR) bands and returns values from −1 to 1. Water can be identified from the MNDWI with values greater than 1 [78]. Equation (1) was used for the calculation of the MNDWI index

$$\text{MNDWI} = \varrho_{\text{Green}} - \varrho_{\text{SWIR}} / \varrho_{\text{Green}} + \varrho_{\text{SWIR}} \quad (1)$$

where ϱ_{Green} is the surface reflectance of the Green band (B3) and ϱ_{SWIR} is the surface reflectance of the SWIR band (B11). Classified images containing the parameters of the Niger River were converted into vector files using the GEE function image. Reduce To Vectors inside GEE. The edge of the flood plain was validated with 35 ground control points distributed along 5 stretches on the right bank and 4 stretches on the left bank, surveyed from 11–21 February 2025 when the flood peaked.

2.4.2. Exposure

The exposed assets were initially identified with participatory mapping sessions during the focus groups with communities. The lack of volunteer-collected information on assets obliged an accurate land use/land cover survey. Consequently, land cover was extracted by visual photo interpretation of freely accessible, high-resolution images on Google Earth (GE) from just before the floods over a 1 km wide strip on each riverside and on all river islands. The spatiotemporal permanence of the assets was verified by observing

their distribution as of January 2014, again using imagery accessible on GE. The assets were then classified by morphology (crop pattern and field size). Twenty-four assets were randomly sampled and visited during the flood that culminated on 16 February 2025 to ascertain the type of buildings and crops. Information on the crop stage of growth, the monetary investments made (seeds, fertilizers, pesticides, fuel for motor pumps, etc.), the yield, price, and where the crop was sold were collected (Figure 1, Table A6).

The crops grown in February 2025 and August 2024 for each field were associated by value and related to the morphology of the fields.

2.4.3. Map Validation

The exposure map was validated first by comparing with the inundated fields as recorded by the Database on Flood in Niger (BDINA) in 2024 [64], and second through 24 ground control points provided by the local agriculture officers.

2.4.4. Assets Value

The damage function for rice crops was expressed in days of crop submergence/growing stage [79], depending on the phenological stage (Table 2).

Table 2. Timing of rice growing stage in Niger [80].

Stages of Rice Crops	Dry Season Week Number	Wet Season Week Number
Seedling	46	25
Nursery	47–52	26–30
Transplanting	1–3	31–33
In plot	4–16	34–48
Harvest	17–19	49–51

However, the local flood carried sediments that silted the crops, resulting in loss. The municipal agricultural officials checked the other crops' flood stage/damage function. Local agriculture officers verified the average yield of each crop per hectare and the average selling price between the harvest price and the maximum price in each municipality, as recorded by the Rural Market Information System [81,82]. The value of each field class exposed to flooding is the weighted average of each crop based on the number of crops grown (Table A7). This value was calculated for each flood. Adobe houses damage is based on the compensation recognized for public works in rural areas [83]. Possible benefits from flooding in terms of additional crops and irrigation fuel savings were investigated (Table A5).

2.5. Risk

The risk was the product of the probability of flooding by the value of the exposed (i) adobe houses, (ii) AHA rice, (iii) pond rice, (iv) horticulture in mid-February, cereals and legumes in mid-August (Figure 5).

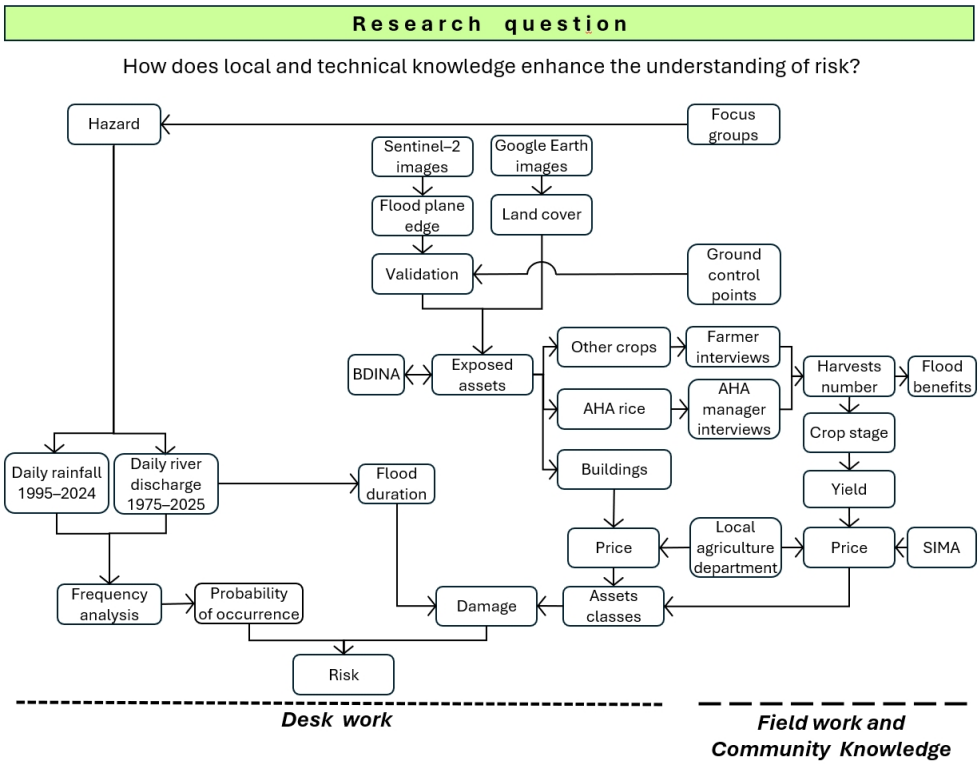

Figure 5. Method flowchart.

3. Results

3.1. Engagement

The first risk mapping step involved the exposed communities, the National Directorate for Meteorology, and the Hydrology Directorate. In this phase, the objectives of risk mapping were explained, the method and timing of the risk analysis were defined, and the contact persons for each community were identified.

3.2. Hazard Identification

Focus groups with the communities of Karma and Namaro, accompanied by participatory mapping, clarified that the flood damage of August 2024 was not caused by the flooding of the Niger River alone. Interviews with the AHA managers highlighted that the Samsire stream broke the embankment in Lata and partially flooded the rice fields. The water could not be evacuated, stagnated for months, and only subsided with evaporation. In Yomadarou, the runoff broke the embankment and flooded it. In the Bani-Te AHA of Kouitoukalé, the flood of the Niger River entered the perimeter from the overflow and inundated the fields. These causes and sources of risk made it necessary to consider the probability of pluvial and fluvial flooding.

3.2.1. Fluvial Flood

Over the last two decades, the local flood peaks increased more than the Guinean flood peaks, with real outliers in 2012, 2020 (historical maximum), and 2024 compared to previous outflows. The return time of the 21 August 2024 flood was estimated to be 12 years (probability 8%), and the event of the 16 February 2025 19 years (probability 5.5%). The local flood of 2024 was the second most extreme in magnitude but with a short duration (95% of the peak was exceeded only one day; 90% of the peak lasted three days). A secondary peak was observed about one month later due to a separate event in the tributaries of the Niger. The Guinean Flood in 2025, with a peak value lower than the local flood, had a much larger

volume and thus inundation potential because it exceeded 95% of the peak for 47 days. For 10 days, water was constantly at the maximum level of 643 cm (Figure 6).

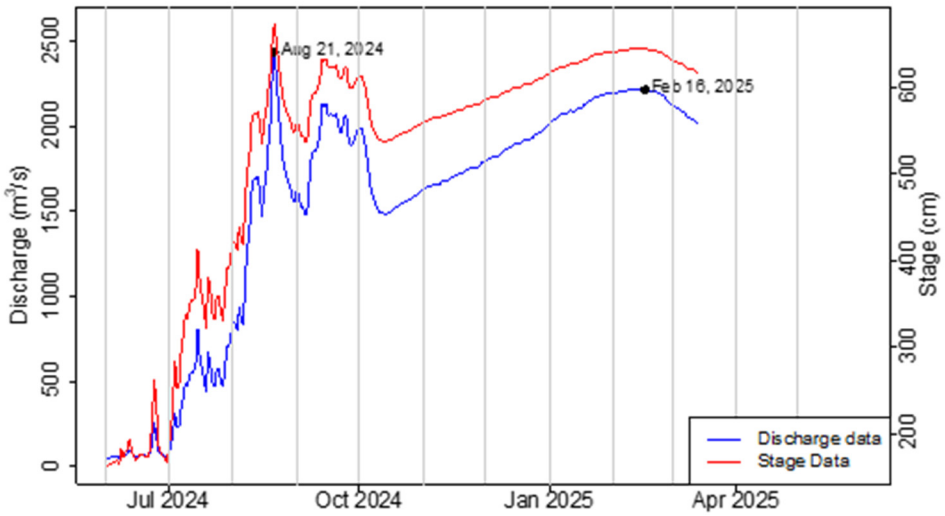

Figure 6. Hydrogram of the Niger River in Niamey from 1 June 2024 to 10 March 2025.

3.2.2. Pluvial Flood

In Karma, on 2–3 August 2024, daily precipitation of 63 mm corresponding to a return time of 2.63 years, equivalent to a probability of 0.38, produced relevant damages. The frequency of the event was estimated based on the historical records at Namaro. The event is close to the annual maximum average and was considered very common. However, it is essential to highlight that on 28 July 2024, a few days before, a slight precipitation of 30 mm occurred, probably saturating the soil and thus reducing the infiltration capacity. Analogously, a damaging 60 mm rainfall occurred at Namaro on 2 August, with a return time of 2.36 years (probability 0.42). This event should not be considered exceptional as it is close to the recorded average.

3.3. Exposed Assets

The flood plain covered 113 km^2 as of 20 August 2024 and 79 km^2 as of 16 February 2025. Twenty-six km^2 were irrigated in a one-kilometer-wide strip along the riverbanks and islands. Most of the crops were in the municipality of Karma, followed by Kourteye (Figures 7–9, Table 3).

Table 3. Agricultural land cover along the river upstream of Niamey.

Municipality	AHA Rice	Pond Rice	Horticulture	Fruits	Tubers	All
	ha	ha	ha	ha	ha	ha
Gothèye	0	20	79	0	0	99
Karma	904	212	271	12		1400
Kourteye	0	469	228	0	2	700
Namaro	299	0	59	0	0	358
All	1203	701	637	12	2	2556

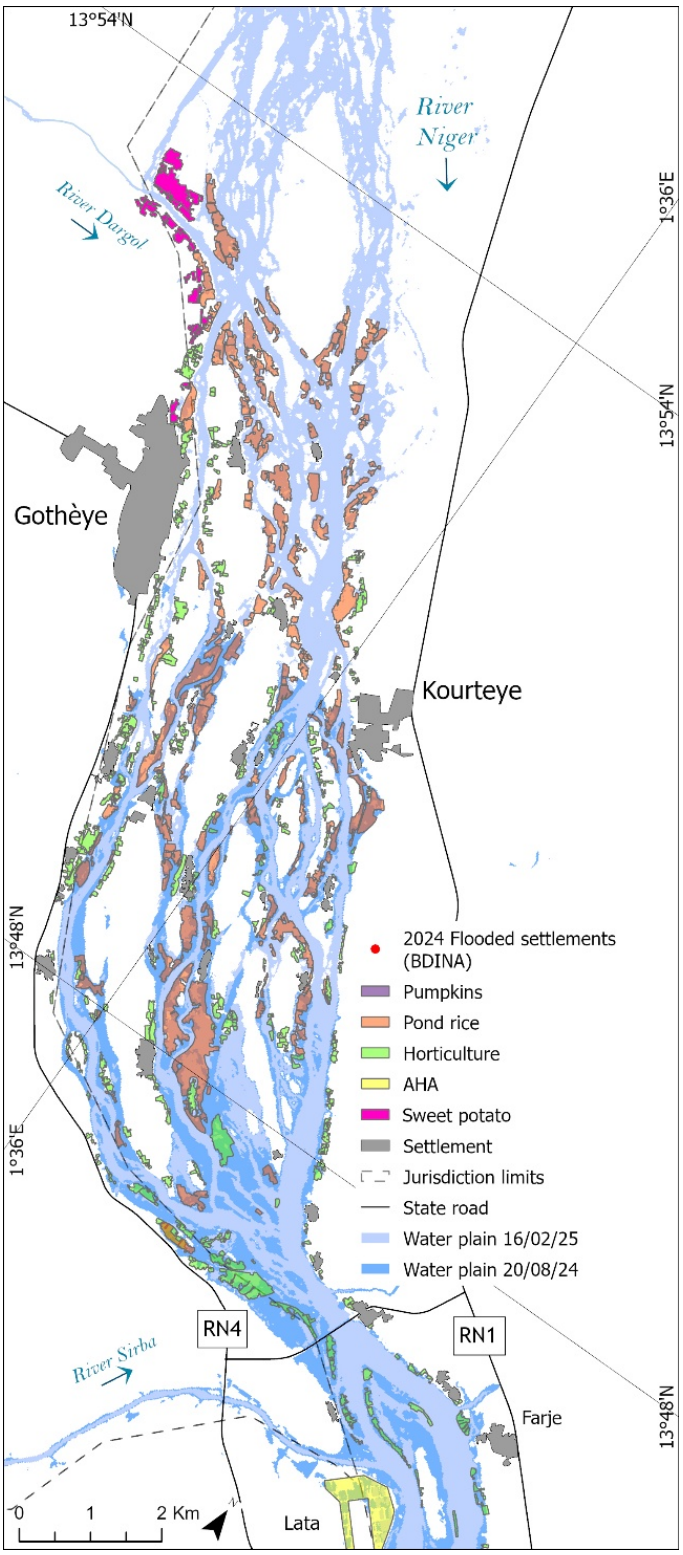

Figure 7. Exposed assets to the floods of 20 August 2024 and 6 February 2025 in the Gotheye-Kourteye sector.

Six classes of assets based on morphology and value were established: adobe houses, AHA rice, pond rice, fruits (pumpkins), tubers (sweet potatoes), and horticulture. Pumpkins were found not to be exposed to flooding, and sweet potatoes were marginally exposed. These classes were discarded in the subsequent risk analysis steps. In mid-February, horticulture consisted of onion (33%), okra (33%), and cassava (33%). In mid-August, these fields were cropped with sorghum (50%), pond rice (30%), and cowpea (20%) (Figure 10).

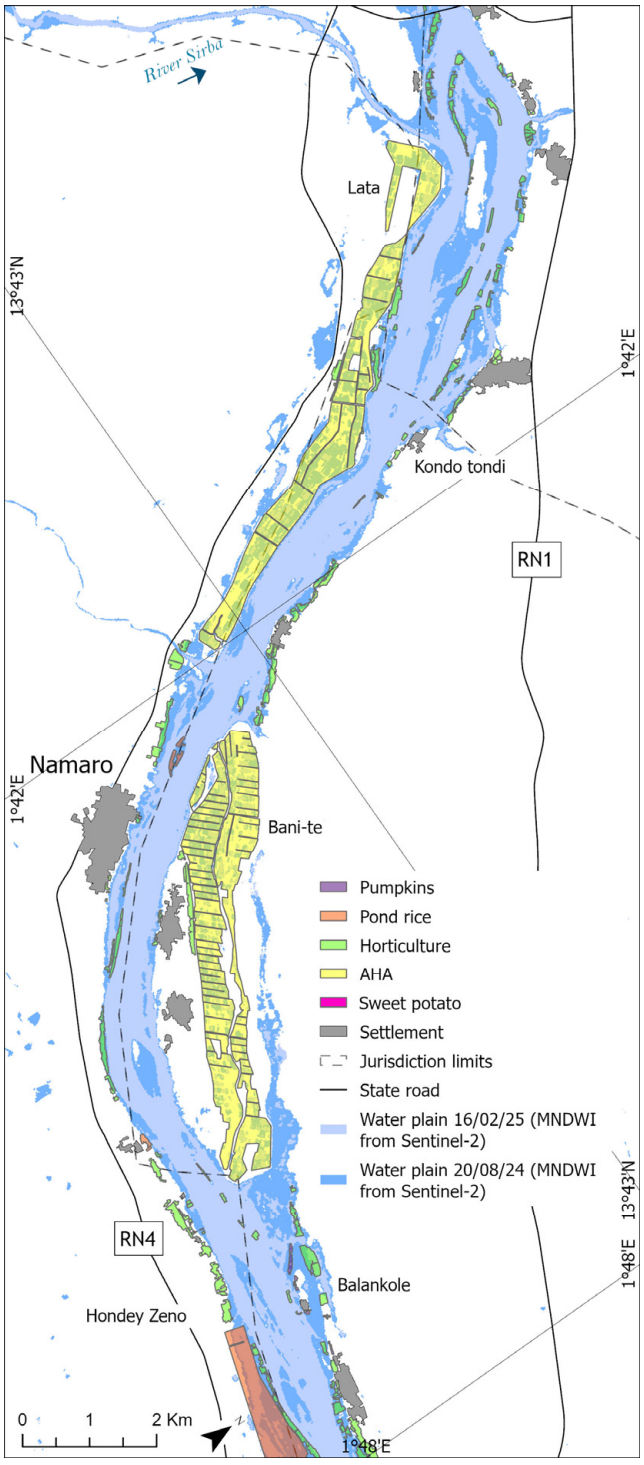

Figure 8. Exposed assets to the floods of 20 August 2024 and 6 February 2025 in the Namaro sector.

The August 2024 flood inundated 730 ha of crops, i.e., 29% of the land under irrigated cultivation. The February 2025 flood inundated 397 ha of crops, i.e., 16% of the land under cultivation. Pond rice was the crop most affected by the local flood, followed by cereals, legumes, and AHA rice. Pond rice was the most affected by the Guinean flood, followed by horticulture. Pumpkins were not flooded. Sweet potatoes were flooded at 0.1 ha only (Table 4).

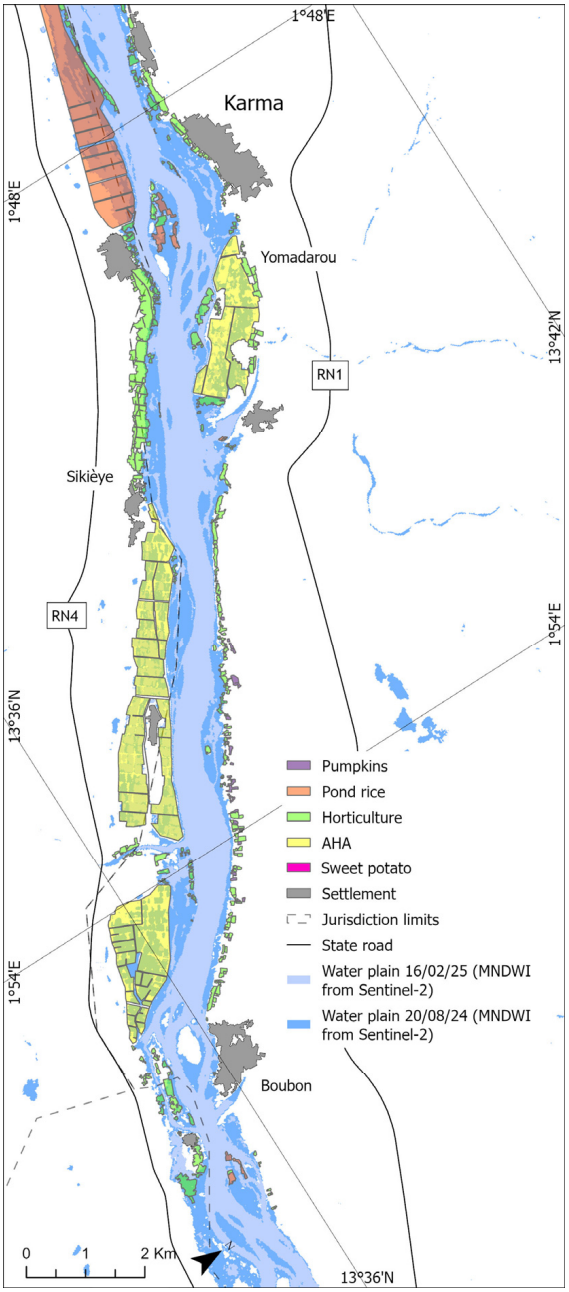

Figure 9. Exposed assets to the floods of 20 August 2024 and 6 February 2025 in the Karma sector.

Table 4. Crops exposure to floods 2024–2025 by municipality.

Flood	Municipality	AHA Rice	Pond Rice	Cereals, Legumes	Horticulture	All
		ha	ha	ha	ha	ha
16 February 2025	Gotheye	0	5	0	10	15
	Karma	0	20	0	25	45
	Kourteye	0	213	0	31	244
	Namaro	0	89	0	3	93
	Total	0	327	0	70	397
21 August 2024	Gotheye	0	6	24	0	30
	Karma	58	50	91	0	199
	Kourteye	0	235	94	0	329
	Namaro	13	128	31	0	172
	Total	71	419	240	0	730

The August flood inundated twenty-one buildings totaling 1517 m^2, mainly in the municipality of Namaro. The February flood did not reach buildings.

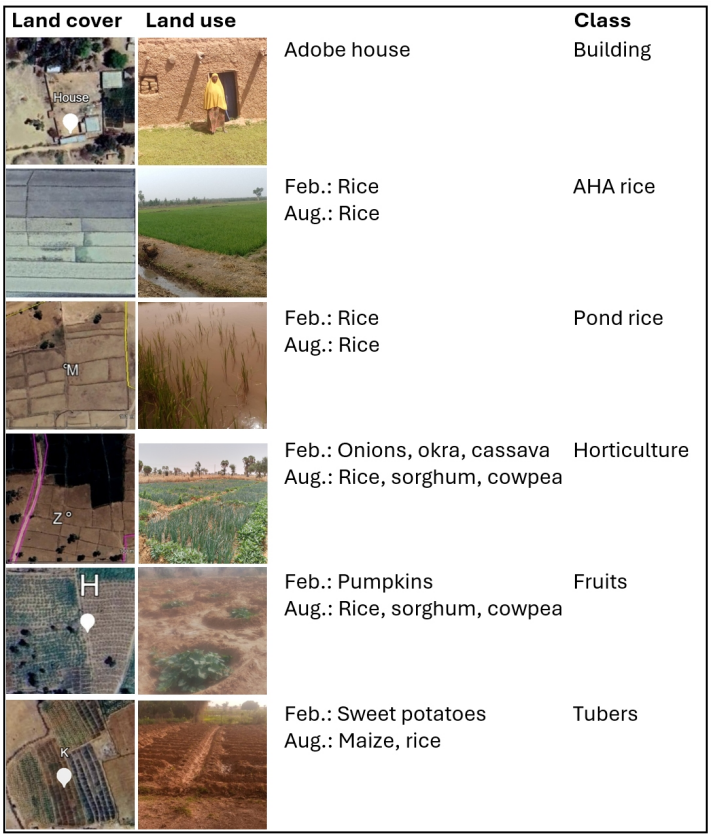

Figure 10. Classes of assets according land cover in February 2024 and ground truth at mid-February 2025. Letters locate the asset in Figure 1.

3.4. Exposure Map Validation

The maps' validation concerns the inundation edge in mid-February 2025 and the asset classes. According to ground truth, the inundated area was always more extensive than the remote sensing detected using MNDWI. At 46% of sites, the gap was under 43 m, and only in four cases did it exceed 127 m (Table 5).

Table 5. Excess of water edge at ground control points over that MNDWI detected in mid-February 2025.

Ground Control Points		Excess of Water Edge at GCP over That MNDWI Detected
Location in Figure 1	**Number**	**Metres**
C	5	323
H	6	83
F	5	36
G	2	170
I (north of)	5	36
J-K	3	150
OLM (north of)	3	40
RS	3	43
T (north of)	5	184
Average	35	127

The exposed assets were compared with those recorded by BDINA in August 2024. BDINA shows an essential discrepancy between municipalities. For example, according to

our analysis, Kourteye had more buildings and agricultural areas flooded but is second to Namaro for buildings and to Karma for crops according to BDINA. At the same time, Namaro, which is third for flooded fields, does not record crop damage according to the BDINA (Table 6).

Table 6. Crop exposure on 21 August 2024, according to the rapid flood map and BDINA.

Municipality	Building Exposure, According to		Crop Exposure, According to	
	Risk Mapping Number	BDINA Number	Risk Map ha	BDINA ha
Gotheye	0	0	30	0
Karma	1	141	199	127
Kourteye	12	155	329	46
Namaro	8	194	172	0
All	21	490	730	173

Consequently, the 24 flooded and non-flooded sites visited validated the exposure map.

3.5. Assets Spatiotemporal Permanence

The AHA irrigation perimeters were created in 1936, 1971, and 1990. A large AHA irrigated perimeter downstream of Namaro was added in 2018 (Figure 11). Between 2014 and 2024, only 15% of the fields were no longer cultivated. The 2020 flood destroyed fifty adobe houses on the river islands.

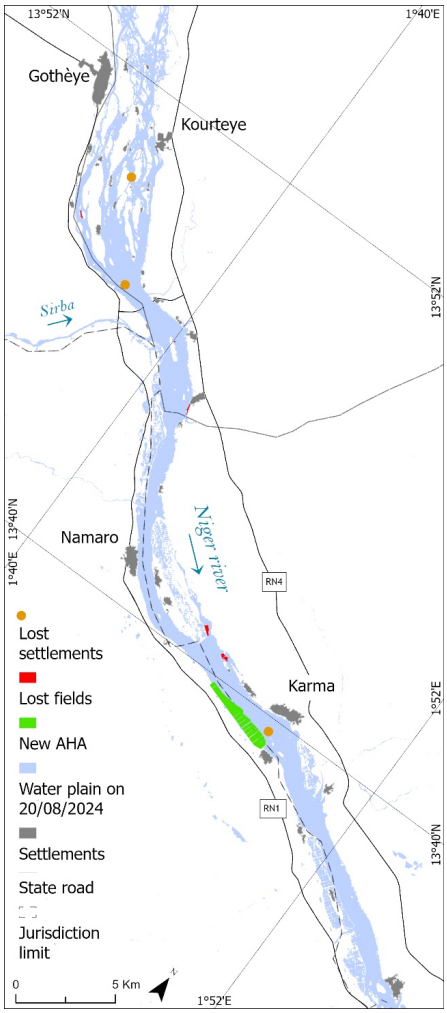

Figure 11. Adobe houses and fields left after January 2014, and new AHAs.

3.6. Damage

As of 20 August 2024, transplanting was in progress in the rice fields. The plants were low, and only slight submergence was needed to lose the crop. Sorghum and cowpea are at leaf out stage. As of 16 February 2025, transplanting was in progress, but the rice fields were not flooded. Onions, okra, cassava, and sweet potato were well-established. However, the ten days of the Guinean flood at peak and the 47 days of its duration at 95% far exceed the crops' resistance to flooding. Therefore, all the flooded crops were considered lost (Table 7).

Table 7. Stage damage for rural crops, according to the municipal agriculture officers.

Crop	Phenological Stage		Submersion Duration		
	Mid-February	Mid-August	Mid-February	Mid-August	Crop Failure After
			Days	Days	Days
Okra	Fructification	Bolting, tillering	10–47		5
Cassava	Early fruiting		10–47		30
Sorghum	-		3	3	5
Cowpea	-		3	3	5
Onion	Bulb		10–47		3–7
Pumpkins	Fructification		10–47		7
AHA rice	-				
Pond rice	Transplanting Leaf out		10–47	30	7–10–15
Sweet potato	Growth		10–47		10
Basilique	Transplanting, growth		10–47		15
Chilli	Fructification		10–47		7

In horticulture, different crops coexist in the same field. Rice is marketed partly just after harvest and partly later when prices peak. Given these complexities, the crop value for each field class was calculated as an average of harvest and maximum prices and a weighted average of crops. Overall, crops and buildings were damaged at EUR 1.112 million, of which EUR 40,000 went to adobe houses, and EUR 1.04 million went from Guinean floods (Table 8).

Table 8. Flood damage upstream of Niamey.

Flood	Assets		Damage	
	Class	ha	EUR/ha	EUR Thousands
Local	Adobe houses	0.1517	260,000	40
	AHA rice	71	2372	168
	Pond rice	419	1424	597
	Cereals, legumes	240	1281	307
	Sum	730		1.112
Guinean	Pond rice	327	1424	466
	Horticulture	70	8200	574
	Sum	397		1040
Hydrological year	Adobe houses		260,000	40
	AHA rice		2372	168
	Pond rice		1424	1063
	Cereals, legumes		1281	307
	Horticulture		8200	574
	Sum	1129	-	2152

The damages per unit area come from [81–85].

Although AHA rice was 29% of the crop inundated by the local flood, it accounted for only 7% of the irrigated crop value. In contrast, pond rice was 82% of the crop inundated by the Guinean flood but 47% in value. Horticulture had a higher value by far.

3.7. Flood Benefits

Interviews with producers from the 24 sites visited, representing all classes of fields, show that the flood did not benefit agriculture in any site.

3.8. Risk

The risk upstream of Niamey was calculated over the hydrological year 2024–2025 as the sum of the local and Guinean flood risk. The global risk is EUR 200,000. Pond rice is at the highest risk (EUR 63,000), followed by AHA rice (EUR 67,000), horticulture (EUR 312,000), and cereals and legumes (EUR 25,000). Horticulture alone accounts for 55% of the mid-February risk, Rice in AHAs accounts for 47%, and adobe houses account for 2% of the mid-August risk (Table 9, Figure 12).

Table 9. Fluvial and pluvial flood risk upstream of Niamey.

Flood	Assets	Hazard	Damage			Risk	
			ha	EUR/ha	EUR Thousands	EUR Thousands	EUR/ha
21 August 2024	Houses	0.08	0.1517	260,000	39.4	3.2	20,800
	AHA rice	0.4	71	2372	168	67.4	28
	Pond rice	0.08	419	1424	597	47.7	114
	Cereals	0.08	240	1280	307	24.6	102
	Sum	-	730			142.8	
16 February 2025	Pond rice	0.055	327	1424	466	25.6	78
	Horticulture	0.055	70	8200	574	31.6	451
	Sum	-	397			57.2	
Hydrological year 2024–2025	Houses	0.08		260,000		3.2	
	AHA rice	0.4		2372		67.4	
	Pond rice	0.08		1424		47.7	
	Pond rice	0.055		1424		25.6	
	Cereals	0.08		1281		24.6	
	Horticulture	0.055		8200		31.6	
	Sum					200.1	

The risk per municipality is highest in Karma EUR 80,000), followed by Kourteye (EUR 68,000), Namaro (EUR 41,000), and Gotheye (EUR 8000) (Table 10).

Table 10. Flood risk by municipality upstream of Niamey.

Flood	Municipality	Asset Class	Hazard	Damage			Risk
				ha	EUR/ha	EUR Thousand	EUR Thousand
21 August 2024	Gotheye	Pond rice	0.08	6	1424	9.5	0.7
		Cereals		24	1281	30.7	2.5
		Sum		30	-	39.3	3.1
	Karma	House	0.38	0.0033	260,000	0.9	0.1
		AHA rice		58	2372	137.6	52.3
		Pond rice		50	1424	71.2	5.7
		Cereals		91	1281	116.6	9.3
		Sum		199	-	362.2	67.4
	Kourteye	House	0.08	0.0451	260,000	11.7	0.9
		Pond rice		235	1424	334.6	26.8
		Cereals		94	1281	120.4	9.6
		Sum		329	-	466.8	37.3
	Namaro	House	0.08	0.1033	260,000	26.9	2.1
		AHA rice	0.42	13	2372	30.8	13.0
		Pond rice		128	1424	182.3	14.6
		Cereals	0.08	31	1281	39.7	3.2
		Sum		172	-	279.7	32.9
	Sum			730		1112.0	140.7

Table 10. *Cont.*

Flood	Municipality	Asset Class	Hazard	Damage			Risk
				ha	EUR/ha	EUR Thousand	EUR Thousand
16 February 2025	Gotheye	Pond rice	0.055	5	1424	7.1	0.4
		Horticulture		10	8200	82.0	4.5
		Sum		15	-	89.1	4.9
	Karma	Pond rice		20	1424	28.5	1.6
		Gardens		25	8200	205.0	11.3
		Sum		45	-	233.5	12.8
	Kourteye	Pond rice		213	1424	303.3	16.7
		Horticulture		31	8200	254.2	14.0
		Sum		244	-	557.5	30.7
	Namaro	Pond rice		89	1424	126.7	7.0
		Horticulture		3	8200	24.6	1.4
		Sum		93	-	151.3	8.3
	Sum			397	-	1031.4	56.7
Hydrological year 2024–2025					-	2143.4	200.1

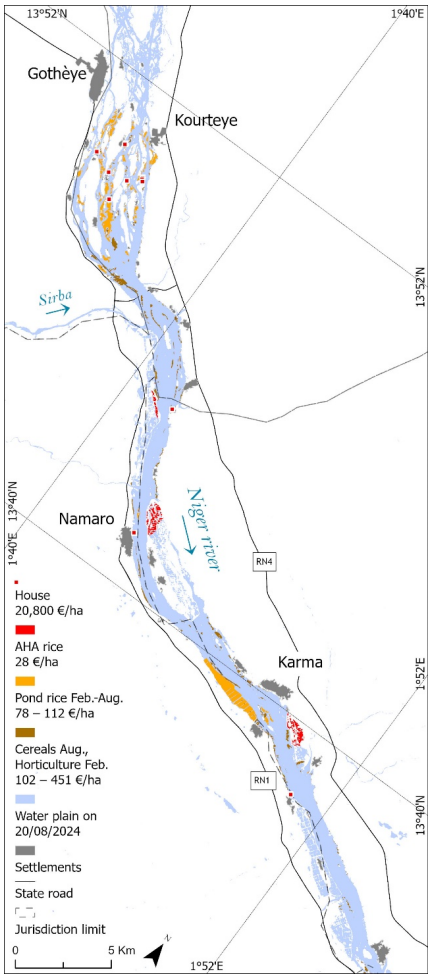

Figure 12. Flood risk map for the hydrological year of 2024–2025.

3.9. Risk Level Interpretation

In risk management, the level of risk precedes the evaluation through residual risk and cost-benefit analyses [62]. The risk level observed along the Niger (EUR 200,000) was low. Nevertheless, the exposed crops were 17% and 31% of the irrigated crop value in mid-February 2025 and mid-August 2025, respectively. Pond rice alone was 47% of all pond rice value in mid-February 2025 and 60% in mid-August 2024. Moreover, all the interviews with the farmers whose fields were in or near the flooded area said that the

ones visited were the only fields cultivated. Crop loss should, therefore, be considered a matter of environmental equity, according to which even a modest level of risk takes on a different meaning.

4. Discussion

The research question was how integrating local and technical knowledge could enhance the understanding of risk hitherto provided by risk mapping in the Global South. We delimited the flood plain during the two floods of the Niger River upstream of Niamey in 2024–2025 using Sentinel-2 images and MNDWI. The floodplain edge was validated following ground control points of its extent at the flood peak in mid-February 2025. Recognizing six asset classes allowed the damage to be estimated and the risk to be expressed in monetary terms. This approach was made possible by closely integrating local knowledge with hydrological, geomatic, and spatial planning knowledge. This brought ten innovations to the risk understanding provided so far:

(i) Early stakeholder participation. Community participation occurs from the methodology definition stage. Communities are not involved as sensors collecting data [86] but for their ability to interpret the observed dynamics and validate the results. This early involvement has implications for the ownership of the mapping, its updating, and future monitoring of local floods.

(ii) Hazard. Heavy rainfall generating flash floods along the minor tributaries of the Niger River breaks the banks of the AHAs, floods the fields, and leads to backwater that cannot drain naturally into the river when it is in flood. Unlike the literature, risk mapping should consider the pluvial and fluvial hazards. The probability of occurrence of the rainfall is about 40%, that of local flood is 8%, and for the Guinean flood is 5.5%. Risk mapping in the Global South rarely expresses hazard as a statistical probability of occurrence [38,46]. The complexity of the processes, as non-stationarities [70,87] or multi-hazards [88], means that risk must be considered qualitatively. This knowledge has three implications. First, the exceptional flood of August 2024 may recur more times in the lifetime of small farmers cultivating along the river. Second, risk reduction measures should consider the reduction of flash floods along the minor tributaries of the Niger River and strengthen the embankments of upstream AHAs in addition to those along the river. Third, a more comprehensive large-scale risk analysis should be developed [89] to link flood risk scenarios with warning thresholds and enable impact-based flood forecasting.

(iii) Assets. Despite literature expectations [90,91], volunteered geographic information contributed to risk mapping with AHAs limits only, corresponding to 10% of the exposed area. Quantitative risk mapping requires more information for each asset (Table A6). The identification of six classes of assets by morphology and value provides information that was previously non-existent in Niger [92]. This information implies the possibility of appreciating the potential damage of the flood to horticulture, which constitutes an essential livelihood for riparian populations.

(iv) Damage complexity. The division of assets into six classes and the assignment of weighted average values in the case of multi-crops and average values in sale prices over the year overcomes this complexity. The estimate of a single cereal crop (rice) prevails in the literature [93]. The implication is a more accurate risk mapping since the value of different asset classes ranges from 1240 EUR/ha (rice) to 8200 EUR/ha on average (onions, okra, and cassava).

(v) Validation. The inundation area at the flood peak in mid-February 2025 is smaller than that measured on the ground. The implication is that damage and risk levels are underestimated. The literature rarely validated the flooded area measured by

satellite imagery with ground control. Usually, the exposure map was validated by comparison with previously inundated sites as they appear from historical satellite imagery [49] or local datasets when available [42]. The significant discrepancy between the inundated areas in August 2024, according to BDINA and our exposure map, led us to prefer ground control points at the edge of the flood plain. However, we observed a significant deviation in the water edge according to the ground control points and satellite images in 17% of the points. This gap has a twofold explanation. First, the satellite images have a resolution of 20 m because the green band to calculate MNDWI is resampled to match the coarser resolution of the shortwave infrared band (Table 1). Second, the areas where the largest deviations are found are cultivated with rice or onions, whose vegetative stage largely obscures the water below.

The method proved fast and accurate, in agreement with [52], and innovative compared to the rapid mapping available in the area today [94,95].

(vi) Spatio-temporal permanence of assets. The fields cultivated in 2024 are stable over time (Figure 11). This character has two implications. The first concerns the validity of the flood risk map over time. To keep the flood risk map current, it will be sufficient to ascertain the crops grown and their selling prices on sample fields. The second implication concerns risk reduction. The omnipresence of irrigated crops along the river and their stability over time affect the opportunity for farmers in the flood zone to move to safer sites. With few exceptions [96], exposure temporality has been poorly investigated.

(vii) Flood benefits. We found no benefits from flooding at any of the 24 sites visited. No flood-recession crops as developed in Tanzania [97], along the Senegal River [98], and in the Dosso region in Niger [99] were found. Neither are wet-season fisheries developed as in the Philippines [100] nor fuel savings for irrigation.

(viii) Risk spatialization. Horticulture is at the highest risk. This result advances knowledge about assets limited to one crop until now [93]. However, comparisons with the literature remain difficult because crops and other rural assets are site-specific. Sometimes, buildings are at the highest risk [34]. At other times, crops are at the highest risk [45]. The numerous settlements along the river and on river islands are marginally at risk. However, the remaining settlements are far from the flooded area. The concentration of risk is in the vicinity of Niamey and on the river islands of Kourteye. These results stand out in the literature on risk mapping, which is rarely practiced with the details proposed in this study. It seldom considers the level of risk by administrative jurisdiction, nor does it locate hot spots. The implication of detailed mapping deals with risk prevention and reduction. This implies that prevention (step back and water pumping) can be directed toward locations where the concentration of damage is most remarkable, such as Sikieye, Kourteye, and Baugawi Zarma.

(ix) Environmental justice. The estimated flood damage is just over EUR two million. According to the flood type, this represents 16% to 29% of the value of all irrigated agriculture in the zone. However, it may have intergenerational and intergroup implications [101] and push small farmers with only their field flooded into greater insecurity [102].

(x) Flood risk scenarios for early warning. Risk maps could be integrated with hydraulic modelling to produce flood risk scenarios [103] linked to flood observations (hydrometers and scales) and hydrological forecasts upstream of the studied area within an early warning system. This will allow forecasting potential risks and damage downstream for each flood level, according to the approach already used for the Sirba local flood early warning system [104].

The hypothesis of achieving a greater understanding of risk through integrating local and technical knowledge than that provided by current risk mapping is confirmed. Focus groups with riparian communities, interviews with AHA managers and farmers, and the involvement of municipal agriculture officers contribute to accurate, participatory, and validated risk mapping. We thus learned about the multi-hazard nature of the flood along the middle Niger River, which until now was narrated as river flooding alone.

However, this study has some limitations. Flood levels are observed downstream of the studied area. Upstream levels should be monitored to contribute to the warning. The damage estimate is approximate because it considers an average between harvest and maximum prices for each crop. For coexisting crops on the same field class, a weighted average is calculated based on the frequency of the crops observed in the sample field.

It is recommended to:

- Install an automatic hydrographic radar station upstream of the Sirba-Niger confluence to intercept the local flood fed by the Dargol River in advance.
- Establish a collaborative protocol with the four riparian municipalities to verify the floodplain edge locally during local and Guinean floods, the crops grown in the sample fields, and feed the exposed assets scenarios accordingly.
- Automate the visualization of potential damage for the benefit of exposed communities and the early flood warning system.
- Extend risk mapping upstream and use Sentinel-1 SAR imagery to overcome the obstacle of cloud cover, which prevents viewing areas inundated by the local flood.

5. Conclusions

In recent years, free access to high-resolution/high-frequency satellite imagery, the spread of hydraulic modelling, and volunteered geographic information have facilitated flood risk mapping in the Global South. However, the maps produced too often stray from the priority of the Sendai Framework for Disaster Risk Reduction 2015–2030, which calls for enhanced participation in disaster preparedness and risk management at the local scale. In three-quarters of reviewed maps, citizen science was sidelined. In the remaining quarter, communities were reduced to sensors collecting data for top-down risk analyses.

We have developed damage-based, quantitative, inclusive flood risk mapping based on local knowledge, integrated by hydrology, geomatics, and spatial planning. We used a bottom-up approach. We started by defining the mapping methodology with the exposed communities. Then, focus groups, interviews with small farmers, and AHA managers interpreted the observed flood dynamics. Remotely sensed information was validated with ground control points by the local agriculture officers.

We demonstrated that an enhanced understanding of risk is possible with a bottom-up approach in mapping. The novelty of this study lies in the participatory approach to risk mapping that produced ten benefits for flood risk management. First, a flood of the Niger River that appeared exceptional may occur more times in the lifetime of riparian farmers. Second, those who farm in a flood zone may have little chance of moving their irrigated crops to a safer site. Third, minor damages after the February 2024 flood (one Million Euros only) can raise a big environmental justice issue. Fourth, the weak points of AHAs are the banks along the river and those inland. Fifth, the potential damages depend on the crop and the season. Sixth, horticulture is the asset at most significant risk during Guinean floods. Seventh, flooding does not bring benefits. Eight, the maps highlight hot spots. Ninth, maps are validated. Tenth, maps can be easily updated and linked to observed flood levels. Participatory risk mapping is not much more time-consuming than top-down rapid flood if risk mapping is based on collaborating with many people with a clear division of roles. This mapping approach cannot estimate risk scenarios that have not previously occurred.

Therefore, it is not an alternative to hydraulic modelling. Nevertheless, by recognizing assets' potential damage, risk mapping can integrate local early warning systems, residual risk, and cost-benefit analyses. The participatory approach to risk mapping described in this study can be replicated in other parts of the River Niger upstream of the studied area and in other contexts in the Global South.

Author Contributions: Conceptualization, M.T.; Methodology, D.G., M.P. and M.T.; Investigation, M.A., M.B., O.B., E.B., G.C., E.F., D.G., M.I.H., G.L.K., F.S. and M.T.; Writing, E.B., D.G., M.T. and V.T.; Writing—review, D.G., V.T. and M.T.; Visualization, G.C. and F.S.; Supervision, M.T.; Funding acquisition, M.T. All authors have read and agreed to the published version of the manuscript.

Funding: This work was supported by the AICS-Italian Agency for Development Cooperation: SLAPIS project (AID 012487).

Data Availability Statement: Data are available in the five tables in the text and the seven tables in Appendix A of the manuscript. Shapefiles are available at https://doi.org/10.17632/m7ds6pkxd3.1.

Acknowledgments: The authors also thank the communities of Karma and Namaro, Moumouni Hassane (Gotheye), Hamadou Ali (Kourteye), Abdoul Kader Amadou Seyni (Karma), and Boubacar Abdou (Namaro) for the fieldwork.

Conflicts of Interest: The authors declare no conflicts of interest.

Appendix A

Table A1. Literature on rapid river flood mapping in the Global South 2017–2024.

Region Country	Images	Flooded Area km^2	Flood Focus	Reference
Gowaingat BG	Sentinel-1/2		Extent, LC	[10]
Nasia GH	Landsat	670	Extent, LC	[11]
White Volta GH	Sentinel-1 SAR	800	Extent, Po, LC	[12]
Gaggar river IN	Sentinel-1 SAR	123	Extent, LC	[13]
Kendrapara IN	RADARSAT SAR	346	Extent, duration	[14]
Purba Medinipur IN	Sentinel-1	240	Extent, LC	[15]
Ganga-Brhama IN		397,707	Extent, LC	[16]
Nilwala LK	Sentinel	109	Extent, LC	[17]
Nsanje MW	Sentinel 1 SAR	90	Extent	[18]
Niger-Benoue NG	MODIS	169,453	Extent, Po	[19]
Niger-Benoue NG	Sentinel-1 SAR	84	Extent, Cr	[20]
Niger delta ML	Landsat	20,000	Extent	[21]
Caprivi NA	Envisat/ASAR	720	Extent	[22]
Cagayan PH	Sentinel-1	551	Extent, Cr, Po	[23]
Sindh, PK	Sentinel-1 SAR	7596	Extent, LC	[24]
Dera Ghazi Khan PK	Landsat	1462	Extent	[25]
Multan PK	Landsat-8	1033	Extent, LC	[26]
SS	Sentinel-1/2, PlanetScope	8649	Extent, cr, bu rds	[27]
Central VN	TerraSAR-X	326	Extent, Cr, Rd, Ut	[28]
Mekong VN	Sentinel-1 SAR	101,000	Extent	[29]

Bu—Buildings; Cr—crops; Rd—Roads; LC—Land cover; Pop—Population: Ut—Utilities.

Table A2. Flood risk map literature in the Global South, 2005–2025.

Region Country	Risk Area km^2	Community Participation	Risk Determinants	Hazard Probability	Risk Expression	Reference
El-Ham AL		None	HV	Indicators	Qualitative	[32]
Rangpur BD	-	None	HV	Indicators	Qualitative	[33]

Table A2. *Cont.*

Region Country	Risk Area km^2	Community Participation	Risk Determinants	Hazard Probability	Risk Expression	Reference
Kalapara BD	51	None	HD	unk	Quantitative	[34]
Southwest BD	-	None	HV	Flood depth	Qualitative	[35]
Niger valley BJ	9118	Exposure	HEV	Indicators	Qualitative	[36]
Adigrat ET	-	None	HV	Indicators	Qualitative	[37]
Edamo ET	161	Flooded zones	HV	Log-Pearson3	Qualitative	[38]
Kobo ET	-	Flood depth	HV	Gumbel	Qualitative	[39]
Moustiques river HT	222	None	HV	Unspecified	Qualitative	[40]
Brahmaputra IN	109	HV interview	HV	Indicators	Qualitative	[41]
Coochbehar IN	3388	None	HV	Indicators	Qualitative	[42]
Navsari IN	2211	V survey	HV	Weibull recurr.	Qualitative	[43]
Narmada IN	99	None	HV	Indicators	Qualitative	[44]
Kashmir IN	581	None	HV	Indicators	Qualitative	[45]
Kosi River IN	-	None	LC, P	Gumbel	Qualitative	[46]
Kosi River IN	1384	None		Indicators	Qualitative	[47]
Nagaon IN	740	None	HV	Flood frequency	Qualitative	[48]
Rel River IN	442	None	HV	no	Qualitative	[49]
Tapi river IN	1463	None	HV	Indicators	Qualitative	[50]
Damansara MY	117	None	HV	Indicators	Qualitative	[51]
Hadejia river NG	30,569	Flood factors, history, validation	HV	Indicators	Qualitative	[52]
Santa Fe PH	12	None	EV	Indicators	Qualitative	[53]
Mono river TG	-	None	HEVC	Indicators	Qualitative	[54]
Mekong VN	3571	None	HV	Flood depth	Qualitative	[55]
Quang Tho VN	-	V	HEV	Indicator	Qualitative	[56]
Quang Binh VN	8065	None	HV	Unspecified	Qualitative	[57]
Quang Binh VN		None	HD	Unspecified	Quantitative	[28]

C—Capacity; D—Damage; E—Exposure; H—Hazard; V—Vulnerability.

Table A3. Focus group with eight members from each exposed municipality (mayor, head of agriculture, livestock, environment, community early warning system emergency response, representative of farmers, women, youth).

Question	
1	Account of the August 2024 flood (date, type, previous day's rainfall, recent rainfall trends, frequency of flooding, extent of flooded areas, threshold of rainfall beginning to cause damage, its trend over time, rainfall dynamics during the flood, how the alert was received, community reaction to the alert, procedure to be followed in the event of an alert, measures put in place, support received after the flood
2	Flood damage (quantification, quantification methods, quantifying body, damage, intangible damage, reason for damage to buildings, replacement costs of buildings, unrepaired damage)
3	Potential measures to cope with flooding (materialization of flood zones, presence of a civil protection officer, most crucial prevention measure implemented, date of implementation, performance of the measure during the flood, further measures to be implemented, measures in the local development plan, speed and direction of the expansion of the settlement

Table A4. Questionnaire submitted to the AHAs managers in February 2025.

Question	
1	Designation of irrigation perimeter
2	Geographical coordinates of the perimeter
3	Photos of the perimeter
4	Year of perimeter creation
5	Area
6	Cultivated area in February 2025
7	Number of fields
8	Number of farmers
9	Type of crop
10	Crop stage as at 20 August 2024
11	Crop stage in mid-February 2025
12	Crop yield T/ha
13	Crop use
14	Sale market
15	Selling price of each crop EUR/100 kg
16	Reason for flooding
17	Lost production (T or EUR) following the flood of 20 August 2024
18	Production lost after the February 2025 flood
19	Measures for preventing future damage
20	Cost of recent similar measures

Table A5. Flood frequency analysis: cumulative distribution function of the GEV with F equal to the non-exceedance frequency and x the peak flood: $F(x) = exp\left[-\left(1-\frac{\theta_3}{\theta_2}(x-\theta_1)\right)^{\frac{1}{\theta_3}}\right]$. With parameters.

	Local Flood	Guinean Flood
θ_1	1708.96	1697.47
θ_2	515.56	246.12
θ_3	0.12	0.163

Rainfall frequency analysis: meta-statistical extreme value distribution equation, assuming that daily precipitation is Weibull-distributed and MEV parameters change over time.

$$\zeta_{MEV}(x) \cong \frac{1}{T}\sum_{j=1}^{T} exp\left[-exp\left(-\frac{y^{w_j}}{C_j^{w_j}} + \ln n_j\right)\right]$$

And parameters:

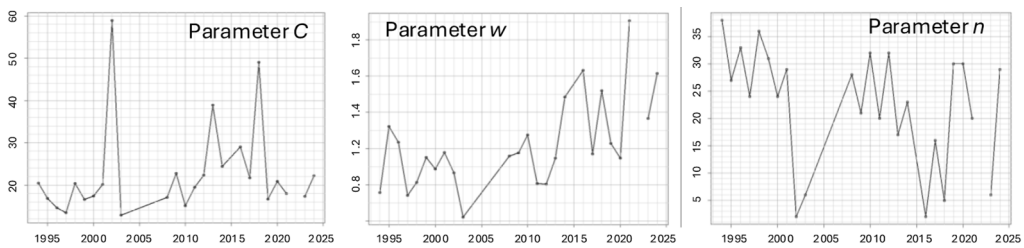

Table A6. Questionnaire per field class submitted to 24 small farmers in mid-February 2025.

Question	
1	Site status as of mid-February 2025 ☐ Flooded. ☐ Not flooded
2	Status of the site in mid-August 2024 ☐ Flooded. ☐ Not flooded
3	Flood duration of the site (days)
4	Number of flood days causing crop loss
5	Flood dates of the pond rice according to the crop calendar
6	Opportunities offered by the flood
7	Crops on-site in mid-February 2025
8	Crop yield (T/ha)
9	Number of harvested crops per year
10	Selling price of each crop EUR/100 kg ☐ At harvest . . .. T/ha. ☐ Max . . .T/ha
11	Market on which production is sold
12	Production costs incurred by the farmer EUR/ha Fertilisers Seeds Pesticides Fuel Sacks Other Total
13	Crops grown on the site in mid-August 2024
14	Crop yield (T/ha)
15	Selling price of each crop EUR/100 kg ☐ At harvest . . .. T/ha. ☐ Max . . .T/ha
16	Market on which production is sold

Table A7. Sale price of the main crops to 2025 in Namaro and Gothèye (EUR).

Crop	Yield	Yields/Year	Price			
			At Harvest	Max	Average	
	T/ha	Number	EUR/100 kg	EUR/100 kg	EUR/100 kg	EUR/ha
AHA Rice N	6–7.5		30	41	36	2430
AHA Rice K	5–7.5		27	46	37	2313
Pond rice	3–5.5		30	37	33.5	1424
Sorghum	5		30	43	37	1850
Cowpea	1.93		34	61	48	926
Onion N	25	1	23	53	38	9500
Cassava N	30	1	19	23	21	6300
Maize	2.49		18	-	18	448
Gombo	20	1	19	69	44	8800
Sweet potato	15	1	11		11	1650
Pumpkin N	35–40	1			27	10,125
Chilli N	2	1	46			920
Basil	2.6	1	5	15	7.5	195
Sesame						

K—Karma, N—Namaro.

References

1. Tramblay, Y.; Villarini, G.; Zhang, W. Observed changes in flood hazard in Africa. *Environ. Res. Lett.* **2020**, *15*, 1040b5. [CrossRef]
2. Panthou, G.; Lebel, T.; Vischel, T.; Quantin, G.; Sane, Y.; Ba, A.; Ndiaye, O.; Diongue-Niang, A.; Diopkane, M. Rainfall intensification in tropical semi-arid regions: The Sahelian case. *Environ. Res. Lett.* **2018**, *13*, 064013. [CrossRef]

3. Tramblay, Y.; Villarini, G.; Saidi, M.E.; Massari, C.; Stein, L. Classification of flood-generating processes in Africa. *Sci. Rep.* **2022**, *12*, 18920. [CrossRef]
4. Descroix, L.; Mahé, G.; Olivry, J.C.; Albergel, J.; Tanimoun, B.; Amadou, I.; Coulibaly, B.; Bouzou Moussa, I.; Faran Maiga, O.; Malam Abdou, M.; et al. Facteurs anthropiques et environnementaux de la recrudescence des inondations au Sahel. In *Les Sociétés Rurales Face aux Changements Climatiques et Environnementaux en Afrique de l'Ouest*; Sultan, B., Lalou, R., Amadou Sanni, M., Oumarou, A., Soumaré, M.A., Eds.; IRD: Marseille, France, 2015; pp. 153–170. ISBN 978-2-7099-2146-6.
5. Wilcox, C.; Vischel, T.; Panthou, G.; Bodian, A.; Blanchet, J.; Descroix, L.; Quantin, G.; Cassséc, C.; Tanimoune, B.; Konee, S. Trends in hydrological extremes in the Senegal and Niger rivers. *J. Hydrol.* **2018**, *566*, 531–545. [CrossRef]
6. United Nations. *Sendai Framework for Disaster Risk Reduction 2015–2030*; UNISDR: Geneva, Switzerland, 2015; Available online: https://www.undrr.org/publication/sendai-framework-disaster-risk-reduction-2015-2030 (accessed on 20 March 2025).
7. Trigg, M.A.; Birch, C.E.; Neal, J.C.; Bates, P.D.; Smith, A.; Sampson, C.C.; Yamazaki, D.; Hirabayashi, Y.; Pappenberger, F.; Dutra, E.; et al. The credibility challenge for global fluvial flood risk analysis. *Environ. Res. Lett.* **2016**, *11*, 094014. [CrossRef]
8. Voigt, S.; Giulio Tonolo, F.; Lyons, J.; Kucera, J.; Jones, B.; Schneiderhan, T.; Platzeck, G.; Kaku, K.; Hazarika, M.K.; Czaran, L.; et al. Global trends in satellite-based emergency mapping. *Science* **2016**, *353*, 247–252. [CrossRef] [PubMed]
9. Shoko, C.; Dube, T. A review of remote sensing of flood monitoring and assessment in southern Africa. *Phys. Chem. Earth* **2024**, *136*, 103796. [CrossRef]
10. Billah, M.; Islam, A.S.; Bin Mamoon, W.; Rahman, M.R. Random forest classifications for land use mapping to assess rapid flood damage using Sentinel-1 and Sentinel-2 data. *Remote Sens. Appl. Soc. Environ.* **2022**, *30*, 100947. [CrossRef]
11. Ghansah, B.; Nyamekye, C.; Owusu, S.; Agyapong, E. Mapping flood prone and Hazards Areas in rural landscape using landsat images and random forest classification: Case study of Nasia watershed in Ghana. *Cogent Eng.* **2021**, *8*, 1923384. [CrossRef]
12. Li, C.; Dash, J.; Asamoah, M.; Sheffield, J.; Dzodzomenyo, M.; Gebrechorkos, S.H.; Anghileri, D.; Wright, J. Increased flooded area and exposure in the Whiter Volta river basin in Western Africa, identified from multi-source remote sensing data. *Sci. Rep.* **2022**, *12*, 3701. [CrossRef]
13. Arora, M.; Sahoo, S.; Bhatt, C.M.; Litoria, P.K.; Pateriya, B. Rapid flood inundation mapping and impact assessment using Sentinel-1 SAR data over Ghaggar River basin of Punjab, India. *J. Earth Syst. Sci.* **2023**, *132*, 183. [CrossRef]
14. Rahman, R.; Thakur, P.K. Detecting, mapping and analysing of flood water propagation using synthetic aperture radar (SAR) satellite data and GIS: A case study from the Kendrapara district of Orissa state of India. *Egypt. J. Remote Sens. Space Sci.* **2018**, *21*, S37–S41. [CrossRef]
15. Khatun, M.; Garai, S.; Sharma, J.; Singh, R.; Tiwari, S.; Rahaman, S.M. Flood mapping and damage assessment due to the super cyclone Yaas using Google Earth Engine in Purba Medinipur, West Bengal, India. *Environ. Monit. Assess.* **2022**, *194*, 869. [CrossRef] [PubMed]
16. Pandey, A.C.; Kaushik, K.; Parida, B.R. Google Earth Engine for large-scale flood mapping using SAR data and impact assessment on agriculture and population of Ganga-Brahmaputra basin. *Sustainability* **2022**, *14*, 4210. [CrossRef]
17. Madhushani, C.I.; Makumbura, R.K.; Basnayake, V.; Pawar, U.; Azamathulla, H.M.; Rathnayake, U. Geospatial assessment of a severe flood event in the Nilwala River basin, Sri Lanka. *Sustain. Water Resour. Manag.* **2024**, *10*, 152. [CrossRef]
18. Gondwe, S.V.C.; Shukla, S.H. Mapping flood risk of Nsanje district in Malawi using Sentinel-1 data. *J. Remote Sens. GIS* **2020**, *11*, 11–34.
19. Nkeki, F.N.; Henah, P.J.; Ojeh, V.N. Geospatial techniques for the assessment and analysis of flood risk along the Niger-Benue basin in Nigeria. *J. Geogr. Inf. Syst.* **2013**, *5*, 123–135. [CrossRef]
20. Odiji, C.; James, G.; Oyewumi, A.; Karau, S.; Odia, B.; Idris, H.; Aderoju, O.; Taminu, A. Decadal mapping of flood inundation and damage assessment in the confluence region of rivers Niger and Benue using multi-sensor data and Google Earth Engine. *J. Water Clim. Change* **2024**, *15*, 348–369. [CrossRef]
21. Bonkoungou, B.; Bossa, A.Y.; van der Kwast, J.; Mul, M.; Sintondji, L.O. Inner Niger delta inundation extent (2010–2022) based on Landsat imagery and the Google Earth Engine. *Remote Sens.* **2024**, *16*, 1853. [CrossRef]
22. Long, S.; Fatoyinbo, E.; Policelli, F. Flood extent mapping for Namibia using change detection and thresholding with SAR. *Environ. Res. Lett.* **2014**, *9*, 035002. [CrossRef]
23. Tumaneng, R.D.; Morico, K.E.R.; Principe, J.A. Remote sensing and Google Earth Engine for rapid flood mapping and damage assessment: A case of typhoon Goni (Rolly) and Vamco (U-lysses). *Int. Arch. Photogramm. Remote Sens. Spat. Inf. Sci.* **2024**, *48*, 445–452. [CrossRef]
24. Ghouri, A.Y.; Rehman, A.; Rasheed, F.; Miandad, M.; Rehman, G. Flood mapping using the Sentinel-1 SAR dataset and application of the change detection approach technique (CDAT) to the Google Earth Engine in Sindh province, Pakistan. *Ecol. Quest.* **2024**, *35*, 149–159. [CrossRef]
25. Sajjad, A.; Lu, J.; Aslam, R.W.; Ahmad, M. Flood disaster mapping using geospatial techniques: A case study of the 2022 Pakistan floods. *Environ. Sci. Proc.* **2024**, *2*, 78. [CrossRef]

26. Sajjad, A.; Lu, J.; Chen, X.; Chisenga, C.; Mazhar, N.; Nadeem, B. Riverine flood mapping and impact assessment using remote sensing technique: A case study of Chenab flood—2014 in Multan district, Punjab, Pakistan. *Nat. Hazards* **2022**, *110*, 2207–2226. [CrossRef]
27. Cian, F.; Delgado Blasco, J.M.; Ivanescu, C. Improving rapid flood impact assessment: An enhanced multi-sensor approach including a new flood mapping method based on Sentinel-2 data. *J. Environ. Manag.* **2024**, *369*, 122326. [CrossRef]
28. Luu, C.; Bui, Q.D.; von Meding, J. Mapping direct flood impacts from a 2020 extreme flood event in Central Vietnam using spatial analysis techniques. *Int. J. Disaster Resil. Built Environ.* **2021**, *14*, 85–99. [CrossRef]
29. Nghia, B.P.Q.; Pal, I.; Chollacoop, N.; Mukhopadhyay, A. Applying Google Earth engine for flood mapping and monitoring in the downstream provinces of Mekong river. *Prog. Disaster Sci.* **2022**, *14*, 10235. [CrossRef]
30. Merz, B.; Thieken, A.H.; Gocht, M. Flood risk mapping at the local scale: Concepts and challenges. In *Flood Risk Management in Europe*; Begun, S., Stive, M.J.F., Hall, J.W., Eds.; Springer: Dordrecht, The Netherlands, 2007; pp. 231–251. [CrossRef]
31. Klaus, S.; Kreibich, H.; Merz, B.; Kuhlmann, B.; Schröter, K. Large-scale, seasonal flood risk analysis for agricultural crops in Germany. *Environ. Earth Sci.* **2016**, *75*, 1289. [CrossRef]
32. Belazreg, N.E.; Habib, S.A.; Sen, Z.; Ferhati, A. Flood risk mapping using multi-criteria analysis (MCA) through AHP method case of El-Ham wadi watershed of Hodna basin (Algeria). *Nat. Hazards* **2024**, *120*, 1023–1039. [CrossRef]
33. Rana, S.M.S.; Habib, A.M.A.; Sharifee, M.N.H.; Sultana, N.; Rahman, S.H. Flood risk mapping of the flood-prone Rangpur division of Bangladesh using remote sensing and multi-criteria analysis. *Nat. Hazards Res.* **2024**, *4*, 20–31. [CrossRef]
34. Islam, F.; Bhattacharya, B.; Popescu, I. Flood risk assessment due to cyclone-induced dike breaching in coastal areas of Bangladesh. *Nat. Hazards Earth Syst. Sci.* **2019**, *19*, 353–368. [CrossRef]
35. Tingsanchali, T.; Karim, M.F. Flood hazard and risk analysis in the southwest region of Bangladesh. *Hydrol. Process.* **2005**, *19*, 2055–2069. [CrossRef]
36. Behanzin, I.D.; Thiel, M.; Szarzynski, J.; Boko, M. GIS-based mapping of flood vulnerability and risk in the Bénin Niger River valley. *Int. J. Geomat. Geosci.* **2015**, *6*, 1653–1669.
37. Nigusse, A.G.; Adhanom, O.G. Flood hazard and Flood risk vulnerability mapping using geo-spatial and MCDA around Adigrat, Tigray region, Northern Ethiopia. *Momona Ethiop. J. Sci.* **2019**, *11*, 90–107. [CrossRef]
38. Edamo, M.L.; Hatiye, S.D.; Minda, T.T.; Ukumo, T.Y. Flood inundation and risk mapping under climate change scenarios in the lower Bilate catchment, Ethiopia. *Nat. Hazards* **2023**, *118*, 2199–2226. [CrossRef]
39. Ayenew, W.A.; Kebede, H.A. GIS and remote sensing based flood risk assessment and mapping: The case of Dikala Watershed in Kobo Woreda Amhara region, Ethiopia. *Environ. Sustain. Indic.* **2023**, *18*, 100243. [CrossRef]
40. Glas, H.; De Maeyer, P.; Merisier, S.; Deruyter, G. Development of a low-cost methodology for data acquisition and flood risk assessment in the floodplain of the river Moustiques in Haiti. *J. Flood Risk Manag.* **2020**, *13*, e12608. [CrossRef]
41. Hazarika, N.; Barman, D.; Das, A.K.; Sarma, A.K.; Borah, S.B. Assessing and mapping flood hazard, vulnerability and risk in the Upper Brahmaputra River valley using stakeholders' knowledge and multicriteria evaluation (MCE). *J. Flood Risk Manag.* **2016**, *11*, S700–S716. [CrossRef]
42. Chakraborty, S.; Mukhopadhyay, S. Assessing flood risk using analytical hierarchy process (AHP) and geographical information system (GIS): Application in Coochbehar district of West Bengal, India. *Nat. Hazards* **2019**, *99*, 247–274. [CrossRef]
43. Patel, S.; Gohil, M.; Pathan, F.; Mehta, D.; Waikhom, S. Assessment of Flood Risk and Its Mapping in Navsari District, Gujarat. *Iran. J. Sci. Technol. Trans. Civ. Eng.* **2023**, *48*, 1021–1028. [CrossRef]
44. Mangukiya, N.K.; Sharma, A. Flood risk mapping for the lower Narmada basin in India: A machine learning and IoT-based framework. *Nat. Hazards* **2022**, *113*, 1285–1304. [CrossRef]
45. Kumar, R.; Acharya, P. Flood hazard and risk assessment of 2014 floods in Kashmir Valley: A space-based multisensor approach. *Nat. Hazards* **2016**, *84*, 437–464. [CrossRef]
46. Sinha, R.; Bapalu, G.V.; Singh, L.K.; Rath, B. Flood risk analysis in the Kosi River basin, North Bihar using multi-parametric approach of Analytical Hierarchy Process (AHP). *J. Indian Soc. Remote Sens.* **2008**, *36*, 335–349. [CrossRef]
47. Kumar, S.; Parida, B.R.; Ahammed, K.K.B. Flood risk assessment of the Kosi River basin in North Bihar using Synthetic Aperture Radar (SAR) data and AHP approach. *Nat. Hazards Res.* 2025; *in press*. [CrossRef]
48. Sharma, S.V.S.P.; Rao, G.S.; Bhanumurthy, V. Development of village-wise flood risk index map using multi-temporal satellite data: A study of Nagaon district, Assam, India. *Curr. Sci.* **2012**, *103*, 25.
49. Jodhani, K.H.; Patel, D.; Madhavan, N.; Gupta, N.; Singh, S.K.; Rathnayake, U. Unravelling flood risk in the Rel River watershed, Gujarat using coupled earth observations, multi criteria decision making and Google Earth Engine. *Results Eng.* **2024**, *24*, 102836. [CrossRef]
50. Chandole, V.; Joshi, G.S.; Srivastava, V.K. Flood risk mapping under changing climate in lower Tapi river basin, India. *Stoch. Environ. Res. Risk Assess.* **2024**, *38*, 2231–2259. [CrossRef]
51. Mojaddadi, H.; Pradhan, B.; Nampak, H.; Ahmad, N.; Ghazali, A.H.B. Ensemble machine-learning-based geospatial approach for flood risk assessment using multi-sensor remote sensing data and GIS. *Geomat. Nat. Hazards Risk* **2017**, *8*, 1080–1103. [CrossRef]

52. Shuaibu, A.; Hounkpè, J.; Bossa, Y.A.; Kalin, R.M. Flood risk assessment and mapping in the Hadejia River basin, Nigeria, using hydro-geomorphic approach and multi-criterion decision-making method. *Water* **2022**, *14*, 3709. [CrossRef]
53. Gacul, L.-A.; Ferrancullo, D.; Gallano, R.; Fadriquela, J.; Mendez, K.J.; Morada, J.R.; Morgado, J.K.; Gacu, J. GIS-based identification of flood risk zone in a rural municipality using fuzzy analytical hierarchy process (FAHP). *Rev. Int. Geomat.* **2024**, *33*, 295–320. [CrossRef]
54. Ntajal, J.; Lamptey, B.L.; Mahamadou, I.B.; Nyarko, B.K. Flood disaster risk mapping in the Lower Mono River Basin in Togo, West Africa. *Int. J. Disaster Risk Reduct.* **2017**, *23*, 93–103. [CrossRef]
55. Dinh, Q.; Balica, S.; Popescu, I.; Jonoski, A. Climate change impact on flood hazard, vulnerability and risk of the Long Xuyen quadrangle in the Mekong Delta. *Int. J. River Basin Manag.* **2012**, *10*, 103–120. [CrossRef]
56. Tran, P.; Shaw, R.; Chantry, G.; Norton, J. GIS and local knowledge in disaster management; a case study of flood risk mapping in Viet Nam. *Disasters* **2008**, *33*, 152–169. [CrossRef] [PubMed]
57. Ha, H.; Bui, Q.D.; Nguyen, H.D.; Pham, B.T.; Lai, T.D.; Luu, C. A practical approach to flood hazard, vulnerability, and risk assessing and mapping for Quang Binh province, Vietnam. *Environ. Dev. Sustain.* **2022**, *25*, 1101–1130. [CrossRef]
58. Scawthorn, C.; Flores, P.; Blais, N.; Seligson, H.; Tate, E.; Chang, S.; Mifflin, E.; Thomas, W.; Murphy, J.; Jones, C.; et al. HAZUS-MH flood loss estimation methodology. II. Damage and loss assessment. *Nat. Hazards Rev.* **2006**, *7*, 72–81. [CrossRef]
59. Kurihara, Y.; Miyamoto, M.; Sunakawa, R. Flood direct damage assessment due to Typhoon Ulysses by satellite images. *Int. J. Disaster Risk Reduct.* **2025**, *118*, 105067. [CrossRef]
60. Tiepolo, M.; Braccio, S.; Fiorillo, E.; Galligari, A.; Katiellou, G.L.; Massazza, G.; Tarchiani, V. Participatory risk assessment of pluvial floods in four towns of Niger. *Int. J. Disaster Risk Reduct.* **2023**, *84*, 103454. [CrossRef]
61. Bennett, M.M.; Gleason, C.J.; Tellman, B.; Alvarez Leon, L.F.; Friedrich, H.K.; Ovienmhada, U.; Mathews, A.J. Bringing satellites down to Earth: Six steps to more ethical remote sensing. *Glob. Environ. Chang. Adv.* **2024**, *2*, 100003. [CrossRef]
62. *IEC/ISO 31010*; International Standard Risk Management—Risk Assessment Techniques. ISO/IEC: Geneva, Switzerland, 2009.
63. *ISO 31000*; 2018 Risk Management. A Practical Guide. ISO: Vernier, Switzerland, 2021.
64. Fiorillo, E.; Maselli, V.; Tarchiani, V.; Vignaroli, P. Analysis of land degradation processes on a tiger bush plateau in South West Niger using MODIS and LANDSAT TM/ETM+ data. *Int. J. Appl. Earth Obs. Geoinform.* **2017**, *62*, 56–68. [CrossRef]
65. Jonkman, S.N.; Bočkarjova, M.; Kok, M.; Bernardini, P. Integrated hydrodynamic and economic modelling of flood damage in the Netherlands. *Ecol. Econ.* **2008**, *66*, 77–90. [CrossRef]
66. De Moel, H.; van Alphen, J.; Aerts, J.C.J.H. Flood maps in Europe—Methods, availability and use. *Nat. Hazards Earth Syst. Sci.* **2009**, *9*, 289–301. [CrossRef]
67. Amirebrahimi, S.; Rajabifard, A.; Mendis, P.; Ngo, T. A framework for a microscale flood damage assessment and visualization for a building using BIM–GIS integration. *Int. J. Digit. Earth* **2016**, *9*, 363–386. [CrossRef]
68. Birkmann, J.; Welle, T. Assessing the risk of loss and damage: Exposure, vulnerability and risk to climate-related hazards for different country classifications. *Int. J. Glob. Warm.* **2015**, *8*, 191–212. [CrossRef]
69. Tiepolo, M.; Braccio, S. Local and scientific knowledge integration for multi-risk assessment in rural Niger. In *Renewing Local Planning to Face Climate Change in the Tropics*; Tiepolo, M., Pezzoli, A., Tarchiani, V., Eds.; Springer: Cham, Switzerland, 2017; pp. 227–245. [CrossRef]
70. Massazza, G.; Bacci, M.; Descroix, L.; Ibrahim, M.H.; Fiorillo, E.; Katiellou, G.L.; Panthou, G.; Pezzoli, A.; Rosso, M.; Sauzedde, E.; et al. Recent changes in hydroclimatic patterns over Medium Niger River basins at the origin of the 2020 flood in Niamey (Niger). *Water* **2021**, *13*, 1659. [CrossRef]
71. Salas, J.D.; Obeysekera, J.; Vogel, R.M. Techniques for assessing water infrastructure for nonstationary extreme events: A review. *Hydrol. Sci. J.* **2018**, *63*, 325–352. [CrossRef]
72. Hosking, J.R.M. L-moments: Analysis and estimation of distributions using linear combinations of order statistics. *J. R. Stat. Soc. Ser. B (Method)* **1990**, *52*, 105–124. [CrossRef]
73. Grimaldi, S.; Kao, S.-C.; Castellarin, A.; Papalexiou, S.-M.; Viglione, A.; Laio, F.; Aksoy, H.; Gedikli, A. Statistical hydrology. In *Treatise on Water Science*; Wilderer, P., Ed.; Academic Press: Cambridge, MA, USA; Elsevier: Oxford, UK, 2011; Volume 2, pp. 479–517.
74. Laio, F.; Ganora, D.; Claps, P.; Galeati, G. Spatially smooth regional estimation of the flood frequency curve (with uncertainty). *J. Hydrol.* **2011**, *408*, 67–77. [CrossRef]
75. Marani, M.; Ignaccolo, M. A metastatistical approach to rainfall extremes. *Adv. Water Resour.* **2015**, *79*, 121–126. [CrossRef]
76. Rahman, S.; Di, L. A systematic review on case studies of remote-sensing-based flood crop loss assessment. *Agriculture* **2020**, *10*, 131. [CrossRef]
77. Notti, D.; Giordan, D.; Calò, F.; Pepe, A.; Zucca, F.; Galve, J.P. Potential and limitations of open satellite data for flood mapping. *Remote Sens.* **2018**, *10*, 1673. [CrossRef]
78. Du, Y.; Zhang, Y.; Ling, F.; Wang, Q.; Li, W.; Li, X. Water bodies' mapping from Sentinel-2 imagery with Modified Normalized Difference Water Index at 10-m spatial resolution produced by sharpening the SWIR band. *Remote Sens.* **2016**, *8*, 354. [CrossRef]

79. Shrestha, B.B.; Okazumi, T.; Miyamoto, M.; Sawano, H. Flood damage assessment in the Pampanga river basin of the Philippines. *J. Flood Risk Manag.* **2016**, *9*, 355–369. [CrossRef]
80. Adamou, H.; Outani, B.A.; Adamou, B.; Yacouba, S.A.; Iliassou, M.M.; Naroua, B.M.; Sodé, C. *Manuel du Système de Riziculture Intensive pour le Riz Irrigué au Niger*; INRAN: Niamey, Niger, 2021.
81. République du Niger (RdN); Ministère du Commerce et de l'Industrie (MCI); Système d'Informations sur les Marchés Agricoles (SIMA). Bulletin Mensuel des Produits Agricoles n. 332 du Mois de Décembre 2024. Available online: https://simaniger.net/wp-content/uploads/2025/01/Bulletin-CR_12_24.pdf (accessed on 20 March 2025).
82. République du Niger (RdN); Ministère du Commerce et de l'Industrie (MCI); Système d'Informations sur les Marchés Agricoles (SIMA). Bulletin Fruits et Legumes 633. Available online: https://simaniger.net/download/bulletin-hebdo-fruits-legumes-semaine-n08-du-mercredi-19-au-mardi-25-fevrier-2025/ (accessed on 20 March 2025).
83. République du Niger (RdN); Ministère de l'Equipment. *Plan Abregé de Reinstallation (PAR) Projet d'Aménagement et Bitumage de la Route Tamaské-Kalfou-Kolloma y Compris la Bretelle Mararraba (63 km)*; Rapport définitif; Direction Générale des Grands Travaux, Direction des Etudes Techniques: Niamey, Niger, 2019; Available online: https://esa.afdb.org/sites/default/files/PAR%20Projet%20d%E2%80%99Am%C3%A9nagement%20Bitumage%20de%20la%20route%20Tamaske-Niger.pdf (accessed on 20 March 2025).
84. RECA. Fiche Technico-économique Riz-hors Aménagement Region Diffa. 2017. Available online: https://reca-niger.org/IMG/pdf/Fiche_technico-economique_riz_Diffa_Mai2017.pdf (accessed on 20 March 2025).
85. RECA. *Analyse Prospective de la Chaine du Valeur du Niebe au Niger 2021–2030*; SOFRECO: Clichy, France, 2022; Available online: https://reca-niger.org/IMG/pdf/l4_etude_niebe.pdf (accessed on 20 March 2025).
86. Wolff, E. The promise of a "people-centred" approach to floods: Types of participation in the global literature of citizen science and community-based flood risk reduction in the context of the Sendai Framework. *Prog. Disaster Sci.* **2021**, *10*, 100171. [CrossRef]
87. Sauzedde, E.; Vischel, T.; Panthou, G.; Tarchiani, V.; Massazza, G.; Ibrahim, M.H. Compound-event analysis in non-stationary hydrological hazards: A case study of the Niger River in Niamey. *Hydrol. Sci. J.* **2025**, *70*, 406–421. [CrossRef]
88. Tiepolo, M.; Bacci, M.; Braccio, S. Multihazard risk assessment for planning with climate in the Dosso region, Niger. *Climate* **2018**, *6*, 67. [CrossRef]
89. Metin, A.D.; Dung, N.V.; Schröter, K.; Vorogushyn, S.; Guse, B.; Kreibich, H.; Merz, B. The role of spatial dependence for large-scale flood risk estimation. *Nat. Hazards Earth Syst. Sci.* **2020**, *20*, 967–979. [CrossRef]
90. McCallum, I.; Liu, W.; See, L.; Mechler, R.; Keating, A.; Hochrainer-Stigler, S.; Mochizuki, J.; Fritz, S.; Dugar, S.; Arestegui, M.; et al. Technologies to support community flood disaster risk reduction. *Int. J. Disaster Risk Sci.* **2016**, *7*, 198–204. [CrossRef]
91. Ward, P.J.; Coughlan de Perez, E.; Dottori, F.; Jongman, B.; Luo, T.; Safaie, S.; Uhlemann-Elmer, S. The need for mapping, modeling, and predicting flood hazard and risk at the global scale. In *Global Flood Hazard. Applications in Modeling, and Forcasting*; Schumann, G.J.-P., Bates, D.B., Apel, H., Aronica, G.T., Eds.; Geophysical Monograph; Wiley: Hoboken, NJ, USA, 2018. [CrossRef]
92. Schulz, D.; Yin, H.; Tischbein, B.; Verleysdonk, S.; Adamou, R.; Kumar, N. Land use mapping using Sentinel-1 and Sentinel-2 time series in a heterogeneous landscape in Niger, Sahel. *ISPRS J. Photogramm. Remote Sens.* **2021**, *178*, 97–111. [CrossRef]
93. Shrestha, B.B.; Kawasaki, A.; Zin, W.W. Development of flood damage functions for agricultural crops and their applicability in regions of Asia. *J. Hydrol. Reg. Stud.* **2021**, *36*, 100872. [CrossRef]
94. Service Régional de Traitement d'Image et de Télédétection (SERTIT). Niger-Tillaberi. Flood-Impact Map Observed the 23/09/2020. 2020. Available online: https://reliefweb.int/map/niger/niger-tillaberi-flood-impact-map-observed-23092020 (accessed on 20 March 2025).
95. United Nations Satellite Centre (UNOSAT). *Niger Niamey and Tillaberi Regions Imagery Analysis 05/10/2022*; Published 10 July 2022 V1; UNOSAT: Geneva, Switzerland, 2022.
96. De Vries, D.H. Temporal vulnerability and the post-disaster 'window of opportunity to woo:' a case study of an African-American floodplain neighborhood after hurricane Floyd in North Carolina. *Hum. Ecol.* **2017**, *45*, 437–448. [CrossRef]
97. Duvail, S.; Hamerlynck, O. The Rufiji river flood: Plague or blessing? *Int. J. Biometeorol.* **2007**, *52*, 33–42. [CrossRef]
98. Bruckmann, L.; Ogilvie, A.; Martin, D.; Diakhaté, F.B.; Tilmant, A. Mapping seasonal flood-recession cropland extent in the Senegal River valley. *Remote Sens. Appl. Soc. Environ.* **2025**, *37*, 101473. [CrossRef]
99. Tarchiani, V.; Fiorillo, E.; Katiellou, G.L.; Tankari, A.M. Risques et opportunités liés aux changements hydrologiques, le cas des mares de Falmey. In *Risque et Adaptation Climatique dans la Region de Dosso au Niger*; Katiellou, G.L., Tarchiani, V., Tiepolo, M., Eds.; L'Harmattan: Paris, France, 2021; pp. 193–212.
100. Juarez-Lucas, A.; Kibler, K.M.; Ohara, M.; Sayama, T. Benefits of flood-prone land use and the role of coping capacity, Candaba floodplains, Philippines. *Nat. Hazards* **2016**, *84*, 2243–2264. [CrossRef]
101. Roy, T.; Hasan, M.K.; Sony, M.M.A.A.M. Climate change, conflict, and prosocial behavior in Southwestern Bangladesh: Implications for environmental justice. In *Environment, Climate, and Social Justice*; Madhanagopal, D., Beer, C.T., Nikku, B.R., Pelser, A.J., Eds.; Springer: Singapore, 2022. [CrossRef]
102. O'Hare, P.; White, I. Beyond 'just' flood risk management: The potential for—and limits to—alleviating flood disadvantage. *Reg. Environ. Change* **2018**, *18*, 385–396. [CrossRef]

103. Massazza, G.; Tamagnone, P.; Wilcox, C.; Belcore, E.; Pezzoli, A.; Vischel, T.; Panthou, G.; Ibrahim, M.H.; Tiepolo, M.; Tarchiani, V.; et al. Flood hazard scenarios of the Sirba River (Niger): Evaluation of the hazard thresholds and flooding areas. *Water* **2019**, *11*, 1018. [CrossRef]
104. Tarchiani, V.; Massazza, G.; Rosso, M.; Tiepolo, M.; Pezzoli, A.; Ibrahim, M.H.; Katiellou, G.L.; Tamagnone, P.; De Filippis, T.; Rocchi, L.; et al. Community and impact based early warning system for flood risk preparedness: The experience of the Sirba River in Niger. *Sustainability* **2020**, *12*, 1802. [CrossRef]